NEW YORK UNIVERSITY
INSTITUTE OF MATHEMATICAL SCIENCES
LIBRARY
4 Washington Place, New York 3, N. Y.

AFCRL-62-704

**NEW YORK UNIVERSITY**
Courant Institute of Mathematical Sciences
Division of Electromagnetic Research

RESEARCH REPORT NO. EM-176

# Geometrical Hydromagnetics

J. BAZER and J. HURLEY

Contract No. AF 19(604)3495

AUGUST, 1962

AFCRL-62-704

New York University
Courant Institute of Mathematical Sciences
Division of Electromagnetic Research

RESEARCH REPORT NO. EM-176

# Geometrical Hydromagnetics

J. Bazer and J. Hurley

August, 1962

Contract No. AF 19(604)3495

Project 5631
Task 563104

Jack Bazer
Jack Bazer

James Hurley
James Hurley

Prepared for: Electronics Research Directorate, Air Force Cambridge Research Labs., Office of Aerospace Research, U. S. Air Force, Bedford, Mass. Reproduction in whole or in part is permitted for any purpose of the U. S. Government.

Requests for additional copies by Agencies of the Department of Defense, their contractors, and other Government agencies should be directed to the:

ARMED SERVICES TECHNICAL INFORMATION AGENCY
DOCUMENTS SERVICE CENTER
ARLINGTON HALL STATION
ARLINGTON 12, VIRGINIA

Department of Defense contractors must be established for ASTIA services or have their 'need-to-know' certified by the cognizant military agency of their project or contract.

All other persons and organizations should apply to the:

U.S. DEPARTMENT OF COMMERCE
OFFICE OF TECHNICAL SERVICES
WASHINGTON 25, D.C.

# TABLE OF CONTENTS

Abstract — page

I. INTRODUCTION — 1

II. THE LINEARIZED EQUATIONS AND THEIR GEOMETRIC SOLUTIONS — 7

III. THE GEOMETRICAL SOLUTION COMPLETED — 20

- A. Rays and Phase Fronts — 20
- B. Variation of the Strength of Fundamental Waves along the Rays — 24
- C. Geometrical Construction of the Phase Fronts. Huygen's Construction. — 27
- D. Fermat's Principle. — 31

IV. PROPAGATION OF ALFVEN AND FAST FRONTS IN INHOMOGENEOUS MEDIA — 33

- A. General Remarks — 33
- B. Propagation of Alfven Fronts in a Dipole Field. — 34
- C. Propagation of Fast Waves in the Earth's Magnetosphere. — 39

V. THE LAWS OF REFLECTION AND REFRACTION — 42

- A. Preliminary Remarks - Snell's Laws — 42
- B. Huygen's Construction of the Scattered Phase Fronts. — 48
- C. The Graphical Method. — 52
- D. General Properties of the Angles of Reflection. — 56
- E. Explicit Formulas for Alfven Waves of a Contact Discontinuity. — 57

APPENDIX I — 62

FIGURES — 65-77

REFERENCES — 78-80

## ABSTRACT

The propagation of small disturbances in an infinitely conducting, perfect, compressible medium is studied from the standpoint of geometrical hydromagnetics. The medium need not be homogeneous. A wave-like time-harmonic disturbance is assumed given on an arbitrary reference surface. Then the various phase fronts (slow, Alfven and fast) which may be thought to evolve out of this surface are obtained as solutions first order partial differential equations. These eikonal-like equations are solved, as in optics, by means of rays, which are shown to satisfy Hamilton's equations and Fermat's principle. The hydromagnetic analogue of Huygen's phase front construction is described. Next, the variation of the disturbance strengths along the rays is determined in terms of the disturbance strengths on the reference surface, to complete the geometrical solution. A noteworthy feature of this solution is that its component modes of propagation, slow, Alfvén and fast, are uncoupled as long as the medium is free of diffracting objects and surfaces of discontinuity. As an illustration of the general theory, the complete geometric solution for the propagation of Alfven disturbances in a dipole field is described with the aid of explicit formulas. Fast wave propagation in various types of inhomogeneous magnetic fields is also briefly discussed. Finally, the problem of reflection and refraction of slow, Alfven and fast disturbances at (possibly curved) surfaces of discontinuity is treated. The hydromagnetic analogues of Snell's laws are derived and their relation to Huygen's wavelet construction is elucidated. It is shown that the introduction of an appropriate set of direction angles for the unperturbed magnetic field (on each side of the discontinuity) 1) reveals the symmetries of "Snell's laws", 2) leads immediately to a simplification of V.C.A. Ferraro's laws relating to the reflection and refraction of Alfven waves and 3) makes possible a simple graphical method for determining the angles and speeds at which the multiply reflected and refracted waves emerge.

# I. INTRODUCTION

In this paper, we present a survey of propagation phenomena in magnetohydrodynamics from the standpoint of "geometrical hydromagnetics". The medium is assumed to be a classical hydromagnetic fluid - that is, perfect, compressible and infinitely conducting. The undisturbed state of this medium is taken to be time-independent; however, special homogeniety is not required so that, in particular, the density and the embedded magnetic field may vary from point to point. The term "geometrical hydromagnetics" is best described at this stage by saying that it bears the same relation to the linearized equations of magnetohydrodynamics as the geometrical optics of crystals bears to Maxwell's equations. As is well-known, there are essentially two geometrical theories. One involves the propagation of discontinuities and pulses, the other involves time-harmonic wave motion. Since the propagation of discontinuities has already been treated by J. Bazer and O. W. Fleischman [1] we confine ourselves here to discussing in detail only spacially continuous, time-harmonic wave motion. Then at the end of Section II, we indicate, following F. G. Friedlander [2a] and D. Ludwig [3] how to include both theories under one general formalism.

Within the context of geometrical hydromagnetics, two basic problems will be treated. Suppose that the disturbance is known to be of the form $\exp\left[i\omega W(\underset{\sim}{x})-(t-t_o)\right]\delta V\,(\underset{\sim}{x},\omega)$, $-\infty < t < \infty$, on a fixed reference surface in space. In this expression, $\omega$ is the angular frequency, $\delta V(\underset{\sim}{x},\omega)$ is a real-valued 7-vector whose components consist of the disturbances in density and in the components of the magnetic and velocity fields, $W(\underset{\sim}{x})$ is an unknown phase function and $t_o$ is any conveniently chosen reference time. It is to be understood here that $W(\underset{\sim}{x}) = 0$ is the equation of the reference surface at time $t_o$. Suppose, in addition, that $\omega$ is large or alternatively that the wave lenths are small in comparison with the significant lengths of the problem. The first problem is to determine the field everywhere when the undisturbed medium is free of boundaries and of discontinuities. The second basic problem involves the reflection and refraction of these small disturbances at curved surfaces of discontinuity in the undisturbed medium.

Sections II and III are devoted to the solution of the first problem. In Section II, it is shown how to decompose the basic disturbance $\exp\left[i\omega W(\underset{\sim}{x})\right]\delta V(\underset{\sim}{x},\omega)$ on the reference surface into three pairs of fundamental disturbances - the so-called slow, Alfven and fast disturbances. Each of these six fundamental disturbances gives rise to wave motions of the form[1] $\exp\left[i\omega(W^{(j)}(\underset{\sim}{x}) - (t-t_o)\right]\delta V^{(j)}(\underset{\sim}{x},\omega)$ $j = 1,2,\ldots,6$, where the $W^{(j)}(\underset{\sim}{x}) - (t-t_o) = 0$ are the equations of the phase fronts which originate at the reference front at time $t = t_o$. The anisotropic character of wave motion, due in part to the motion of the undisturbed medium and in part to the presence of a magnetic field, is evidenced by the fact that the propagation speeds of these phase fronts are direction-dependent.

---

[1] We neglect terms of order $\omega^{-1}$ and higher. It is, however, possible in principle to carry out the analysis to arbitrary order in $\omega^{-1}$.

A method for constructing the phase functions $W^{(j)}$, $j = 1,2,\ldots,6$ is presented in Section III where the ordinary differential equations for the "rays" associated with each mode of propagation are derived. The analogues at Huygens' phase front construction, Fermat's principle, Fresnel's ray surface and reciprocal surface of phase front normals are discussed. As in the geometrical optics of crystals, the rays are the conveyors of the "energy in a given mode".[2] It is essentially this fact, specifically the conservation of this "energy" along a tube of rays, that enables one to determine how each of the $\delta V^{(j)}(\underset{\sim}{x},\omega)$ behaves as $\underset{\sim}{x}$ varies, thereby completing the geometric solution of the first problem.

The fact that the amplitudes $\delta^{(j)}V(\underset{\sim}{x},\omega)$ can be determined deserves to be underscored. In geometrical optics, for example, it has been known for a long time that the transition from wave optics to geometrical optics involves asymptotic expansions which lead to methods for constructing the phase fronts such as have been described above. Not so well known, however, is the fact that the geometrical theory enables one to determine the propagation of the amplitudes. A systematic exploitation of this possibility was initiated by R. K. Luneberg [4] only twenty years ago and has been elaborated and extended with great success in the papers of M. Kline [5a-c] and J. B. Keller [6a-6c].

As in geometrical optics, the geometric solution can be obtained even when the method of seperation of variables fails. Of even greater significance in practical applications is that each of the six fundamental wave motions propagate independently of one another. When, by contrast, one attempts to solve linearized equations of magnetohydrodynamics exactly, one finds that the six modes will, in general, be coupled. Coupling of the geometric modes does, however, take place when a phase front, be it slow, Alfven or fast, is incident on a surface of discontinuity in the undisturbed medium. Then one finds, as a rule, that each type of incident wave produces three refracted and three reflected waves. Section V is devoted to the discussion of the laws governing the reflection and refraction of the various types of incident modes. It is shown that the introduction of an appropriate set of direction angles for the magnetic fields (see Figure 7) makes possible an effective graphical procedure for determining the angles of reflection and refraction and leads to a simplification of V.C.A. Ferraro's [7] laws of reflection and refraction for Alfven waves. We also explain the relation of this graphical procedure to Huygens' classical construction of reflected and refracted wave fronts.

---

[2] The precise meaning of this phrase will be given later.

The theory of Sections II and III is illustrated in Section IV with the aid of several concrete examples. In all cases, the medium is assumed to be motionless but otherwise arbitrary. The section begins with the proof of somewhat surprising property of Alfven wave propagation, namely, that the strength of a disturbance on an Alfven front is independent of the local geometry of the front. Specifically, it is shown that the strength of an Alfven disturbance varies as the fourth root of the density along a ray and is independent of the so-called expansion ratio (see equation (3.21)). This result means, among other things, that the propagation of Alfven fronts into a region in which the rays converge need not be accompanied by an intensification of the distrubance. In fact, in the case of constant density, the disturbance is constant along a ray. Next to be considered is the problem of Alfven wave propagation in a dipole field. Here, we give explicit formulas, up to a single quadrature, for the motion of the phase fronts. This quadrature, it may be added, is easily evaluated in the case of constant density. Finally, we derive formulas for the propagation of fast fronts into various types of inhomogeneous magnetic fields.

By introducing suitable "diffracted rays" and systematically applying the methods of J. B. Keller and co-workers (see reference [6a]), one may extend geometrical hydromagnetics to cover the effects of diffraction. Experience with the corresponding extension of geometrical optics (see [6a]) indicates this theory will be accurate to wavelengths as large as the diameter of the diffracting object. The application of the geometrical theory is also limited at the high frequency end of the spectrum, owing to the failure of the equations of hydromagnetism. Derivations of the single-fluid equations with a scalar conductivity from the two-fluid theory point to the following restrictions. (1) The impressed frequency $\nu = (\omega/2\pi)$ must be much less than the electron gyro-frequency $\nu_e$, the plasma frequency $\nu_p$, and the frequency of collision $\nu_c$ between the two species of particles; (2), the relation $\nu_e << \nu_c$ must hold. Then the additional requirement that the displacement current be negligible in comparison with the conduction current guarantees the validity of the hydromagnetic equations. It is not claimed here that these are the weakest or minimum number of restrictions; depending on the mode in question and its direction of propagation some of these may be relaxed considerably (see references [26], [27], and [28]).

A brief survey of the relevant literature is given at the end of Section II.

## II. THE LINEARIZED EQUATIONS AND THEIR GEOMETRIC SOLUTIONS

In the absence of disturbances, it is assumed that the medium is undergoing steady isentropic flow so that this flow is governed by

$$
\begin{array}{ll}
\nabla \cdot \underset{\sim}{H} = 0, & A_0 \\
\nabla \times (\underset{\sim}{H} \times \underset{\sim}{u}) = 0, & \underset{\sim}{A}_1 \\
\rho(\underset{\sim}{u} \cdot \nabla)\underset{\sim}{u} + a^2 \nabla \rho + \mu \underset{\sim}{H} \times (\nabla \times \underset{\sim}{H}) = 0, & \underset{\sim}{A}_2 \\
\nabla \cdot (\rho \underset{\sim}{u}) = 0, & A_3 \\
S = \text{const (independent of } \underset{\sim}{x} \text{ and } t). & A_4
\end{array}
\tag{2.1}
$$

In these equations, $\underset{\sim}{H}$ is the magnetic intensity, $\underset{\sim}{u}$ is the fluid velocity, $\rho$ is the density, a is the speed of sound, $\mu$ is the specific magnetic inductive capacity, and S is the entropy per unit mass. MKS units are used throughout. We prefer to ignore gravitational terms here and in the body of our analysis. However, in Section IIIB we list the few changes in the final results that are necessitated by the inclusion of such terms. The (time-dependent) linearized system is:

$$
\begin{array}{lll}
0 = L_0(\delta \underset{\sim}{H}) & = \nabla \cdot \delta \underset{\sim}{H}, & \delta A_0 \\
0 = \underset{\sim}{L}_1(\delta \underset{\sim}{H}, \delta \underset{\sim}{u}) & = \delta \underset{\sim}{H}_t + \nabla \times (\delta \underset{\sim}{H} \times \underset{\sim}{u}) + \nabla \times (\underset{\sim}{H} \times \delta \underset{\sim}{u}), & \delta \underset{\sim}{A}_1 \\
0 = \underset{\sim}{L}_2(\delta \rho, \delta \underset{\sim}{u}, \delta \underset{\sim}{H}) & = \rho\, \delta \underset{\sim}{u}_t + \rho(\underset{\sim}{u} \cdot \nabla)\delta \underset{\sim}{u} + \rho\, (\delta \underset{\sim}{u} \cdot \nabla)\underset{\sim}{u} & \delta \underset{\sim}{A}_2 \\
 & \quad + \mu \underset{\sim}{H} \times (\nabla \times \delta \underset{\sim}{H}) + \nabla (a^2\, \delta \rho) & \\
 & \quad + \delta \rho(\underset{\sim}{u} \cdot \nabla)\underset{\sim}{u} + \mu \delta \underset{\sim}{H} \times (\nabla \times \underset{\sim}{H}), & \\
0 = L_3\, (\delta \rho, \delta \underset{\sim}{u}) & = \delta \rho_t + \nabla \cdot (\underset{\sim}{u}\, \delta \rho) + \nabla \cdot (\rho\, \delta\, \underset{\sim}{u}), & \delta A_3 \\
0 = \delta S\,. & & \delta A_4
\end{array}
\tag{2.2}
$$

In these equations, $\delta \underset{\sim}{H}$, $\delta \underset{\sim}{u}$, $\delta \rho$ and $\delta S$ denote small variations of $\underset{\sim}{H}$, $\underset{\sim}{u}$, $\rho$ and S. $L_0$, $\underset{\sim}{L}_1$, $\underset{\sim}{L}_2$ and $L_3$ are abbreviations for the linear differential operators appearing in the last members of $\delta A_0$, $\delta \underset{\sim}{A}_1$, $\delta \underset{\sim}{A}_2$, and $\delta A_3$; the subscript t signifies partial differention with respect to time.

Forming the relation

$$\mu \delta \underset{\sim}{H} \cdot \underset{\sim}{L}_1 + \delta \underset{\sim}{u} \cdot \underset{\sim}{L}_2 + \frac{a^2}{\rho} \delta \rho L_3 = 0, \tag{2.3}$$

by multiplying $\delta \underset{\sim}{A}_1, \delta \underset{\sim}{A}_2$ and $\delta A_3$ by $\delta \underset{\sim}{H} \cdot$, $\delta \underset{\sim}{u} \cdot$ and $a^2 \delta \rho / \rho$, we obtain after some manipulation the "energy" equation

$$\begin{aligned} 0 = {} & \mathcal{E}_t + \nabla \cdot \underset{\sim}{F} + \rho \delta \underset{\sim}{u} \cdot (\delta \underset{\sim}{u} \cdot \nabla) \underset{\sim}{u} - \frac{\mu}{\rho} \delta \rho \delta \underset{\sim}{u} \cdot [\underset{\sim}{H} \times (\nabla \times \underset{\sim}{H})] \\ & + \mu \delta \underset{\sim}{u} \cdot [\delta \underset{\sim}{H} \times (\nabla \times \underset{\sim}{H})] - \frac{1}{2} \frac{\delta \rho^2}{\rho} \underset{\sim}{u} \cdot \nabla (a^2) + \frac{1}{2} \mu \delta H^2 \nabla \cdot \underset{\sim}{u} \\ & - \mu \delta \underset{\sim}{H} \cdot (\delta \underset{\sim}{H} \cdot \nabla) \underset{\sim}{u}, \end{aligned} \tag{2.4}$$

where the "energy"[3] $\mathcal{E}$ is defined by

$$\mathcal{E} = \tfrac{1}{2} \rho \delta u^2 + \tfrac{1}{2} \mu \delta H^2 + \tfrac{1}{2} \frac{a^2}{\rho} \delta \rho^2, \tag{2.5}$$

and the "flux of energy" or system "flux" is defined by

$$\underset{\sim}{F} = \mathcal{E} \underset{\sim}{u} + a \delta \rho \delta \underset{\sim}{u} + \mu (\underset{\sim}{H} \times \delta \underset{\sim}{u}) \times \delta \underset{\sim}{H}. \tag{2.5'}$$

The last term in equation (2.6) will be recognized as the Poynting vector, since in fluid of infinite conductivity the electric field is given by the expression $\mu \underset{\sim}{H} \times \delta \underset{\sim}{u}$. The first term in the right member of (2.6) gives the energy density transported due to the motion of the fluid and the second term is the ordinary flux term of acoustics.

Geometrical hydromagnetics enters the picture when one asks for a solution of the system (2.2) which is a superposition of waves of the form

---

[3] $\mathcal{E}$ should not be confused with the second order energy term obtained by expanding the expression for the total energy of the nonlinear system. In addition to terms such as those appearing in $\mathcal{E}$, the second order energy contains terms involving second variations.

$$(\delta\underset{\sim}{H},\ \delta\underset{\sim}{u},\ \delta\rho) = e^{i\omega[W(\underset{\sim}{x})-(t-t_o)]}\sum_{n=0}^{\infty}\left(\frac{1}{i\omega}\right)^n(\delta\underset{\sim}{H}^{(n)},\ \delta\underset{\sim}{u}^{(n)},\ \delta\rho) \qquad (2.6)$$

Here $\omega$ denotes the angular frequency, $W(\underset{\sim}{x})$ denotes an unknown *phase function* and $\delta\underset{\sim}{H}^{(n)}$, $\delta\underset{\sim}{u}^{(n)}$, $\delta\rho^{(n)}$, $n = 1, 2, \ldots,$ denote unknown *amplitudes*. These amplitudes are required to be real apart from a common phase factor of unit amplitude and to be independent of $\omega$ and $t$. It is not required that the infinite sum converge, merely that it be asymptotic in some sense to the exact solution for large $\omega$ or small $\lambda$.

For a fixed instant of time,

$$W(\underset{\sim}{x}) - (t - t_o) = k_o$$

is for each constant $k_o$ the equation of a *surface of constant phase* or *phase front*. To complete the formulation of the problem, it is necessary to specify $\delta\underset{\sim}{H}^{(n)}$, $\delta\underset{\sim}{u}^{(n)}$ and $\delta\rho^{(n)}$ $n = 0, 1, 2, \ldots,$ on some conveniently chosen phase front. We choose for this purpose the phase front $\mathcal{S}(t_o)$ defined by

$$\mathcal{S}(t_o) : \quad W(\underset{\sim}{x}) = 0 \qquad (2.7)$$

and write

$$(\delta\underset{\sim}{H},\ \delta\underset{\sim}{u},\ \delta\rho)\Bigg|_{\mathcal{S}(t_o,} = \sum_{n=0}^{\infty}\left(\frac{1}{i\omega}\right)^n(\delta\underset{\sim}{H}_o^{(n)},\ \delta\underset{\sim}{u}_o^{(n)},\ \delta\rho_o^{(n)}) \qquad (2.8)$$

for the form of the disturbance on $\mathcal{S}(t_o)$.

One may approach the problem of determining the unknown amplitudes and phase function $W(\underset{\sim}{x})$ in either of two ways. One may seek to determine the unknown amplitudes on fixed phase fronts $W(\underset{\sim}{x}) = \text{const}$ in space or follow a given phase front, e.g. $\mathcal{S}(t)$ defined by

$$\mathcal{S}(t) : \quad W(\underset{\sim}{x}) - (t - t_o) = 0, \qquad (2.9)$$

from the time $t_o$ that it evolves out of $\mathcal{S}(t_o)$ and seek to determine the unknown amplitudes on $\mathcal{S}(t)$. We shall adopt the second point of view.

As already observed in the introductory section, an arbitrarily polarized wave on $\mathcal{S}(t_o)$ gives rise to three pairs of phase fronts, slow, Alfven and fast. Each of these six fronts carries a disturbance of the form (2.6). Since the amplitudes of each distrubance wave can be determined independently of the others, we automatically achieve the separation of wave motions referred to in Section I.

The velocity of the phase front $\mathcal{S}(t)$ is defined to be the velocity along the orthogonal trajectories to the family of phase fronts, $W(\underset{\sim}{x}) - (t-t_o) = 0$. Employing this definition one finds that[4]

$$\underset{\sim}{U} = \underset{\sim}{n} / |\nabla W| \tag{2.10}$$

where $\underset{\sim}{n}$ is the unit normal to the phase front so that

$$\underset{\sim}{n} = \nabla W / |\nabla W|. \tag{2.11}$$

If we substitute the right member of equation (2.7) into equations (2.2) $\delta A_0$ - (2.2) $\delta A_3$ and equate the powers of $\omega$, we obtain the following recursive system:

$$\left\{ \begin{aligned} \underset{\sim}{n} \cdot \delta \underset{\sim}{H}^{(0)} &= 0, \\ (M - \rho^{\frac{1}{2}} c\, I)\, \delta R^{(0)} &= 0; \end{aligned} \right. \tag{2.12}$$

$$\left\{ \begin{aligned} \underset{\sim}{n} \cdot \delta \underset{\sim}{H}^{(k)} &= - U L_o(\delta \underset{\sim}{H}^{(k-1)}), \\ (M - \rho^{\frac{1}{2}} c\, I) \delta R^{(k)} &= P(\delta R^{(k-1)}), \quad k = 1, 2, \ldots \end{aligned} \right. \tag{2.13}$$

In equation (2.13), M is the symmetric 6 × 6 matrix

---

[4] Let $\underset{\sim}{x} = \underset{\sim}{X}(t)$ be one such trajectory. Then we find that $\underset{\sim}{U} = \frac{d\underset{\sim}{x}}{dt}$ and $W(\underset{\sim}{X}(t)) - (t - t_o) = 0$ (identically). Differentiating this last equation, we conclude that $U = |\nabla W|^{-1}$.

$$M = \left[\begin{array}{cccc|cc} 0 & \mu^{\frac{1}{2}}H_y & -\mu^{\frac{1}{2}}H_n & 0 & 0 & 0 \\ \mu^{\frac{1}{2}}H_y & 0 & 0 & a\rho^{\frac{1}{2}} & 0 & 0 \\ -\mu^{\frac{1}{2}}H_n & 0 & 0 & 0 & 0 & 0 \\ 0 & a\rho^{\frac{1}{2}} & 0 & 0 & 0 & 0 \\ \hline 0 & 0 & 0 & 0 & 0 & -\mu^{\frac{1}{2}}H_n \\ 0 & 0 & 0 & 0 & -\mu^{\frac{1}{2}}H_n & 0 \end{array}\right] \qquad (2.14)$$

$\delta R^{(k)}$ is the column vector

$$\delta R^{(k)} = \left[ \left(\frac{\mu}{\rho}\right)^{\frac{1}{2}}\delta H_y^{(k)},\ \delta u_n^{(k)},\ \delta u_y^{(k)},\ \frac{a}{\rho}\delta\rho^{(k)},\ \delta u_z^{(k)};\ \delta H_z^{(k)} \right]; \qquad (2.15)$$

$P(\delta R^{(k-1)})$ is the column vector

$$P(\delta R^{(k-1)}) = -U\sqrt{\rho}\left[\left(\frac{\mu}{\rho}\right)^{\frac{1}{2}} \bar{L}_{1,y}^{(k-1)},\ \rho^{-1}\bar{L}_{2,n}^{(k-1)},\ \rho^{-1}\bar{L}_{2,y}^{(k-1)},\ \frac{a}{\rho}\bar{L}_{3}^{(k-1)}, \right. \qquad (2.16)$$

$$\left. \rho^{-1}\bar{L}_{2,z}^{(k-1)} \quad \left(\frac{\mu}{\rho}\right)^{\frac{1}{2}}\bar{L}_{1,z}^{(k-1)} \right]$$

and

$$c = U - u_n \qquad (2.17)$$

is the disturbance speed (relative to the flow velocity in the direction normal to the wave front). The operators $\bar{L}_1, \ldots \bar{L}_3$ appearing in equation (2.16) are the same as the $L_1, \ldots L_3$ that appear in (2.2) except that the time-derivative operators have been deleted. The second subscript on the vector operators indicates which component is intended.

The particularly simple form of M is the result of choosing a local system of coordinates on $\mathcal{S}(t)$ such that the x-axis is directed along $\underset{\sim}{n}$ and the y-axis is directed along $\underset{\sim}{H} - (\underset{\sim}{H} \cdot \underset{\sim}{n})\underset{\sim}{n}$.

We shall henceforth be concerned only with the lowest order terms in the solution (2.6). This means that we are required to find the solutions of the zero-th order equations (see equation (2.12)). With the aid of the remaining equations one may, in principle, obtain the first and higher order terms; however the problems that one encounters in practice do not as yet seem to warrant such refinement.

We begin by observing that $\delta R^{(0)}$ is necessarily an eigenvector of M. Since M is symmetric it has a complete set of six real-valued mutually orthogonal eigenvectors. To find these, we first determine the eigenvalues $\rho^{\frac{1}{2}}c$ from the secular equation

$$0 = \det\,(M - \rho^{\frac{1}{2}} c\, I) = (\rho c^2 - H_n^2)\,[(\rho c^2 - \rho a^2)(\rho c^2 - \mu H_n^2) - \rho c^2 (H^2 - H_n^2)]. \qquad (2.18)$$

The solutions of this equation evidently occur in pairs $\pm$ c, c > 0. Let

$$c_A = b_n = (\mu\, H_n^{\,2}\, \rho^{-1})^{\frac{1}{2}} \qquad (2.19)$$

- the so-called Alfven disturbance speed - be the non-negative zero of the first factor and $c_s (c_{slow})$ and $c_f (c_{fast})$ be the smallest and largest of the non-negative zeroes of the second factor, in the last member of equation (2.18). Then, it is found that

$$\frac{c_s}{b} = \left\{ \frac{1}{2}(1 + r) - \tfrac{1}{2}\,[(1 + r)^2 - 4r \cos^2 \chi]^{\frac{1}{2}} \right\}^{\frac{1}{2}}, \qquad (2.20)$$

$$\frac{c_f}{b} = \left\{ \frac{1}{2}(1 + r) + \tfrac{1}{2}\,[(1 + r)^2 - 4r \cos^2 \chi]^{\frac{1}{2}} \right\}^{\frac{1}{2}}, \qquad (2.21)$$

and that

$$0 \le c_s \le \min\{a, b_n\} \le \max\{a, b_n\} \le c_f.$$

where r and b are defined by

$$r = a^2/b^2 \tag{2.22}$$

$$b = \sqrt{\mu H^2 \rho^{-1}}, \tag{2.23}$$

and $\chi$ is the angle between $\underset{\sim}{H}$ and $\underset{\sim}{n}$. Figure 1 is a polar diagram of $c_s/b$, $c_A/b$ and $c_f/b$ against $\chi$. The figure, which is plotted for the parameter value $r = 1/2$ is typical of those in the entire parameter range $r \leq 1/2$. Representative curves associated with values of r in the ranges $1/2 < r < 1$, $r = 1$, $1 < r < 2$, $2 < r$ are given in the report [1 a].

Let it be supposed, for the present, that $\underset{\sim}{n}$ is neither parallel nor perpendicular to $\underset{\sim}{H}$. Substituting the appropriate value of c into equation (2.12) and solving for the components of $\delta R^{(0)}$, we find that $\delta H^{(0)}$, $\delta u^{(0)}$ and $\delta \rho^{(0)}$ in Alfven, slow and fast waves are given by the following formulas:

Alfven:

$$\begin{aligned} \delta \underset{\sim}{H}^{(0)} &= \pm (\epsilon/E^{\frac{1}{2}})\, \underset{\sim}{n} \times \underset{\sim}{H}, \\ \delta \underset{\sim}{u}^{(0)} &= -\, \epsilon(\mu H_n/E^{\frac{1}{2}} \rho b_n)\, \underset{\sim}{n} \times \underset{\sim}{H}, \\ \delta \rho^{(0)} &= \delta S^{(0)} = 0; \\ E^{\frac{1}{2}} &= \sqrt{\rho}\; b\, |\sin \chi|. \end{aligned} \tag{2.24}$$

Slow and Fast:

$$\begin{aligned} \delta \underset{\sim}{H}^{(0)} &= -\, (\epsilon/E^{\frac{1}{2}})\underset{\sim}{n} \times (\underset{\sim}{n} \times \underset{\sim}{H}), \\ \delta \underset{\sim}{u}^{(0)} &= \mp \frac{\epsilon}{E^{\frac{1}{2}}} \left[ c\left(\frac{b_n^2}{c^2} - 1\right)\underset{\sim}{n} - \frac{\mu H_n}{\rho c}\, \underset{\sim}{n} \times (\underset{\sim}{n} \times \underset{\sim}{H})\right], \\ \delta \rho^{(0)} &= -\, \frac{\epsilon}{E^{\frac{1}{2}}}\, \rho \left(\frac{b_n^2}{c^2} - 1\right) \end{aligned} \tag{2.25}$$

$$E^{\frac{1}{2}} = \sqrt{\rho}\, b|\sin \chi| \left\{\left|\frac{2(c^2/b^2)-(1+r)}{(c^2/b^2)-r}\right|\right\}^{\frac{1}{2}} =$$

$$\frac{\sqrt{\rho}\, b^3}{c^2}\left\{ |(c^2/b^2) - \cos^2\chi| \left[(c^2/b^2)-(1+r))\right]\right\}^{\frac{1}{2}}.$$

In equation (2.25), c is $c_s$ or $c_f$ according as to the wave is slow or fast. There are two solutions associated with each of the speeds $c_A$, $c_s$ and $c_f$, one corresponding to motion of the phase front along $\underset{\sim}{n}$ (upper signs) and the other corresponding to motion in the opposite direction (lower signs) along $-\underset{\sim}{n}$. The E's are normalization constants, having the dimensions of energy per unit volume, which are fixed by requiring that $\rho/2$ times the square of the Euclidean length of the vector $\delta R^{(0)}$ be equal to $\epsilon^2$ - in symbols (see equations (2.15) and (2.5))

$$\tfrac{1}{2}\rho\, \delta R^{(0)} \cdot \delta R^{(0)} \equiv \tfrac{1}{2}(\rho\, \delta u^{(0)})^2 + \tfrac{1}{2}\frac{a^2}{\rho}(\delta\rho^{(0)})^2 + \tfrac{1}{2}\mu\,(\delta H^{(0)})^2 = \epsilon^2. \quad (2.26)$$

The quantity $\epsilon$, which is evidently dimensionless, is called the *strength* of the wave. Measured is units of E, *$\epsilon^2$ is the energy per unit volume in the wave* (see footnote 3). In order that the linearization on which the entire analysis is based be valid, it is necessary that $|\epsilon|$ be a small quantity initially and remain so subsequently.

The analogues of equations (2.24) and (2.25) for the thus far excluded directions of $\underset{\sim}{n}$ may be obtained as follows: Rotate $\underset{\sim}{n}$ into the direction parallel (or normal) to $\underset{\sim}{H}$ keeping the direction of $\underset{\sim}{n} \times \underset{\sim}{H}$ fixed. Then calculate the limits approached by the expressions for $\delta\underset{\sim}{H}^{(0)}$, $\delta\underset{\sim}{u}^{(0)}$ and $\delta\rho^{(0)}$. The resulting limits are the desired formulas as may be verified by substituting the appropriate components into the eigenvalue equation (2.12).

By direct calculation, it can be shown with the aid of equation (2.18) that

$$\tfrac{1}{2}\,\rho(\delta u^{(0)})^2 = \tfrac{1}{2}\,\frac{a^2}{\rho}\,(\delta\rho^{(0)})^2 + \tfrac{1}{2}\,\mu\,(\delta H^{(0)})^2 = \tfrac{1}{2}\,\epsilon^2 \qquad (2.27)$$

in all waves, slow, Alfven and fast. Thus, the energy density associated with each of the fundamental modes is divided in equal parts between the kinetic energy density on one hand and the magnetic and internal energy densities on the other[5].

Suppose $\underset{\sim}{n} \times \underset{\sim}{H} \neq 0$ and that $\underset{\sim}{n}$ and $\underset{\sim}{H}$ are in the plane of the page. Then, a glance at equations (2.24) and (2.25) reveals, the magnetic vector $\delta\underset{\sim}{H}$ is polarized perpendicular or parallel to the plane of the page according as the front is an Alfven front or not. In all cases, $\delta\underset{\sim}{H}$ is parallel to the phase front and its direction is determined by $\underset{\sim}{n}$ and $\underset{\sim}{H}$.

The problem of determining the disturbance evolving out of a given initial disturbance may now be reduced to the corresponding problem for the six fundamental modes. Let $\underset{\sim}{x}$ be a point on the phase front $\mathcal{S}(t_0)$ and let $\underset{\sim}{n}(\underset{\sim}{x})$ be the unit normal at $\underset{\sim}{x}$. Corresponding to each such $\underset{\sim}{x}$ and $\underset{\sim}{n}(\underset{\sim}{x})$, let $R^{\pm}_{s,0} = R^{\pm}_{s,0}(\underset{\sim}{x},\underset{\sim}{n})$, $R^{\pm}_{A,0} = R^{\pm}_{A,0}(\underset{\sim}{x},\underset{\sim}{n})$, $R^{\pm}_{f} = R^{\pm}_{f,0}(\underset{\sim}{x},\underset{\sim}{n})$ be the six mutually orthogonal eigenvectors of the matrix M. Without loss of generality it may be assumed that these vectors are of unit length[6]. Then, ignoring all but the lowest order terms in the right member of (2.8), we may decompose the initial disturbance into the six fundamental waves as follows:

---

[5] The internal energy density vanishes in Alfven waves.

[6] The components of these unit vectors may be obtained from equations (2.24) and (2.25) simply by setting $\epsilon = 1$.

$$\begin{aligned}\delta D(\underset{\sim}{x}) &= \left[\left(\frac{\mu}{\rho}\right)^{\frac{1}{2}} \delta H_y,\ \delta u_n,\ \delta u_y,\ \frac{a\delta\rho}{\rho},\ \delta u_z,\ \left(\frac{\mu}{\rho}\right)^{\frac{1}{2}} \delta H_z\right] \\ &= \sum_j \left(\epsilon^+_{j,0}\, R^+_{j,0} + \epsilon^-_{j,0}\, R^-_{j,0}\right) \qquad (2.28) \\ &= \sum_j \left(\delta D^+_j(\underset{\sim}{x}) + \delta D^-_j(\underset{\sim}{x})\right)\end{aligned}$$

Here $\underset{\sim}{x}$ is any point on $\mathcal{S}(t_0)$ and j takes on the "values" s, A and f and $\delta D^\pm_j(\underset{\sim}{x}) = \epsilon^\pm_{j,0}\, R^\pm_{j,0}$. Since the $R^\pm_{j,0}$ are unit vectors, the $\epsilon^\pm_{j,0}$ measure the strengths of the fundamental waves in the above decomposition. If $\delta D(\underset{\sim}{x})$ is complex-valued then, as the $R^\pm_{j,0}$ are real, the $\epsilon^\pm_{j,0}$ will be complex-valued. However, we shall show at the end of Appendix I that only the amplitudes of the $\epsilon^\pm_{j,0}$ change on the phase fronts $\mathcal{S}^\pm_j(t)$ $j = s, A, f$, which evolve out of $\mathcal{S}(t_0)$. The distinction between real and complex $\epsilon^\pm_j$ is therefore not an essential one.

We have thus far ignored what may be termed contact fronts. Contact fronts do not propagate relative to the underlying flow. In addition, they may carry a disturbance $\delta S$ in the entropy S. No special consideration is required for contact waves that appear as limiting cases of the slow, fast and Alfven modes. However, if it is desired to take into account contact fronts that are not connected to the fundamental modes by means of of a limiting process, it is necessary to increase the number of components in $\delta D$ and $R^\pm_j$, $j =$ s, A, f by one and to add an entropy vector $\epsilon_c R_c$ to the sum (3.28). To obtain the components of $R_c$ one simply substitutes the right member of equation (2.8) into (2.2) and looks for a solution in which $c = U - u_n$ vanishes.

Much of the work on the propagation of continuous time-harmonic disturbances in a compressible hydromagnetic medium has been concerned with the derivation of exact solutions for various simple geometries. The contributions of N. Herlofson [8], H. C. van de Hulst [9], S. Lundquist [10], A. Banos, Jr. [11], to mention a few of the earlier papers, are examples of such work. Herlofson and van de Hulst were the first to note the existence of essentially three distinct disturbance speeds (of equations (2.19) - (2.21)). The more recent asymptotic results of M. J. Lighthill [12] are geometrical in character but valid only when the undisturbed state of the medium is spacially homogeneous as well as time-independent. In the reports [13], [14], K. O. Friedrichs and H. Kranzer called attention to hyperbolicity of the linearized hydromagnetic equations - a property that it shares with the linearized equations of gas dynamics and Maxwell's equations. In addition, they took the first steps in exploiting the analogies between these systems. Among other results they described the wave forms emanating from a weak localized disturbance in a uniform medium and catalogued the various fundamental wave motions. The propagation of weak hydromagnetic disturbances was discussed by J. Bazer and O. W. Fleischman in their report [1a] and paper [1b]. It should be noted that this paper dealt with propagation in inhomogeneous media. In [15] H. Grad discusses continuous wave motion in a uniform media. Among other things, he shows that in more than one dimension the fundamental waves can only be partially separated, in contrast to the complete separability of the geometrical modes. Grad shows however, that special solutions can be constructed which propagate at one of the above mentioned disturbance speeds (relative to the flow). The reader is referred to the review article by G. F. J. MacDonald [16] for a survey of geophysical applications of hydromagnetic wave propagation and for additional bibliographical material. The paper [17] by A. J. Dessler and E. N. Parker on the hydromagnetic theory of geomagnetic storms should also be consulted in this connection.

A comparison of the formulas (2.24) and (2.25) for the six fundamental propagating modes with the corresponding formulas for the jumps across weak shocks (cf. [1b] p. 268 and [13] pp. 14-20.) reveals that they are the same apart from a constant multiplier. That this is to be expected may be seen from the following. Note that the fundamental asymptotic expansion (2.7) has the form

$$(\delta \underset{\sim}{H}, \delta \underset{\sim}{u}, \delta \rho) = \sum_{n=0}^{\infty} f_n(\varphi(\underset{\sim}{x},t))\,(\delta \underset{\sim}{H}^{(n)}, \delta \underset{\sim}{u}^{(n)}, \delta \rho^{(n)}) \qquad (2.29)$$

where $\varphi(\underset{\sim}{x},t) = W(\underset{\sim}{x}) - (t - t_o)$ and $\qquad (2.30)$

$$\begin{aligned} f_o &= \exp(i\omega s) \\ f_n &= \int f_{n-1}(s)\,ds \end{aligned} \qquad (2.31)$$

Now it is easily verified that the right member of equation (2.29) is a formal solution of equation (2.2) for arbitrary $f_o(s)$, provided $f_n$ is defined as in (2.31). This function may in fact be highly singular, e.g. a delta function or, more generally, a distribution in the sense of L. Schwartz [29]. If, in particular, one chooses $f_o(s)$ to be a function which takes the value 1 within the boundary of a disturbance and zero outside, one is led to the theory of Bazer and Fleishman [1a, b] and to the formulas (2.24) and (2.25) for the fundamental propagating modes.

Formal expansions of the above type were first introduced by F. G. Friedlander in his study [2a] of propagation phenomena in acoustics. D. Ludwig [3] has employed similar expansions in his treatment of the initial value problem for hyperbolic systems. This work contains the most comprehensive treatment to date of various mathematical questions which arise in the rigorous theory of such expansions. The earlier papers by R. Courant and P. D. Lax [18] R. Lewis [19] and P. D. Lax [20], (particularly the last of two) also bear directly on the problem under discussion.

Much of the material described in the last two paragraphs may be regarded, as an outgrowth of the work on geometrical optics by R. K. Luneberg [2], on geometrical acoustics by J. B. Keller [6b] and on general hyperbolic equations by M. Kline [5]. The present work is to a large extent patterned after the work of these three authors. An informative historical account of the evolution of the geometric method has been given by M. Kline [5c]. Among other things, the relation of the geometrical method to the W.K.B. method is explained in this paper.

Finally, it should be mentioned that M. J. Lighthill [12], F. G. Friedlander [2b] and H. Weitzner [21] have derived expressions for the far fields due to various types of point sources in a homogeneous medium.

## III. THE GEOMETRICAL SOLUTION COMPLETED

### A. Rays and Phase Fronts

Setting

$$\underset{\sim}{p} = \nabla W , \qquad p = |\nabla W| \tag{3.1}$$

we find, employing the definitions of $\underset{\sim}{n}$, U and c (see equations (2.10), (2.11) and (2.17)), that

$$\underset{\sim}{n} = p^{-1}\underset{\sim}{p} , \qquad U = p^{-1} \tag{3.2}$$

$$c = p^{-1} - (\underset{\sim}{u} \cdot \underset{\sim}{p})p^{-1} \tag{3.3}$$

The vector $\underset{\sim}{p}$ is called the *phase normal*.

In this notation, we may re-express the determinantal equation (3.3) as

$$0 = \mathcal{H}(\underset{\sim}{x},\underset{\sim}{p}) = \prod_{i=1}^{3} \mathcal{H}_i^{+}(\underset{\sim}{x},\underset{\sim}{p})\, \mathcal{H}_i(\underset{\sim}{x},\underset{\sim}{p}), \tag{3.4}$$

where

$$\mathcal{H}_i^{\pm}(\underset{\sim}{x},\underset{\sim}{p}) = (\underset{\sim}{u} \cdot \underset{\sim}{p} - 1) \pm p\, c_i(\underset{\sim}{x}, \underset{\sim}{n}). \qquad i = 1,2,3. \tag{3.5}$$

The quantities $c_1$, $c_2$ and $c_3$ are the disturbances speeds $c_A$, $c_s$ and $c_f$ respectively. The functions $\mathcal{H}$, $\mathcal{H}_1^{\pm}$, $\mathcal{H}_2^{\pm}$ and $\mathcal{H}_3^{\pm}$ will be referred to as the *total*, *Alfven*, *slow* and *fast* Hamiltonians respectively for reasons which will be clear presently. Since by definition $\underset{\sim}{p} = \nabla W$, each of the six equations

$$\mathcal{H}_i^{\pm}(\underset{\sim}{x},\underset{\sim}{p}) = 0 \tag{3.6}$$

is a first order partial differential equation. As is well known, the problem of solving such equations may be reduced to that of solving a system of ordinary differential equations of the first order in $(\underset{\sim}{x},\underset{\sim}{p})$

space. The rays are the curves in $\underset{\sim}{x}$-space obtained by solving this system of equations. If the time t is employed as the curve parameter then the ray equations corresponding to each of the above Hamiltonians are simply Hamiltons' equations of motion with $\underset{\sim}{x}$ and $\underset{\sim}{p}$ serving as space and momentum variables, respectively. Employing this fact we are led to the following set of ray equations (cf [1b] p. 371):

± Alfven rays:

$$\frac{d\underset{\sim}{x}}{dt} = \underset{\sim}{u} \pm (\mu/\rho)^{\frac{1}{2}} \operatorname{sgn} (\underset{\sim}{H} \cdot \underset{\sim}{p})\, \underset{\sim}{H} \equiv \underset{\sim}{v}_A^{\pm}, \qquad \text{(a)}$$

$$\begin{aligned} \frac{d\underset{\sim}{p}}{dt} = {} & -(\underset{\sim}{p} \cdot \nabla)\left[ \underset{\sim}{u} \pm (\mu/\rho)^{\frac{1}{2}} \operatorname{sgn} (\underset{\sim}{H} \cdot \underset{\sim}{p})\, \underset{\sim}{H}\right] \\ & - \underset{\sim}{p} \times \left\{\nabla \times \left[\underset{\sim}{u} \pm (\mu/\rho)^{\frac{1}{2}} \operatorname{sgn} (\underset{\sim}{H} \cdot \underset{\sim}{p})\, \underset{\sim}{H}\right] \right\}, \qquad \text{(b)} \end{aligned} \qquad (3.7)$$

± slow rays:

$$\frac{d\underset{\sim}{x}}{dt} = \underset{\sim}{u} \pm c_s \underset{\sim}{n} \pm \frac{b^2 r(H_n/H^2)}{c_s(\underset{\sim}{x},\underset{\sim}{n})Q(\underset{\sim}{x},\underset{\sim}{n})}(\underset{\sim}{H} - H_n \underset{\sim}{n}) = \underset{\sim}{v}_s^{\pm}, \qquad \text{(a)}$$

$$\frac{d\underset{\sim}{p}}{dt} = -(\underset{\sim}{p} \cdot \nabla)\, \underset{\sim}{u} - \underset{\sim}{p} \times (\nabla \times \underset{\sim}{u}) \mp p \nabla c_s, \qquad \text{(b)} \qquad (3.8)$$

± Fast rays:

$$\frac{d\underset{\sim}{x}}{dt} = \underset{\sim}{u} \pm c_f \underset{\sim}{n} \mp \frac{b^2 r\, (H_n/H^2)}{c_f(\underset{\sim}{x},\underset{\sim}{n})\, Q(\underset{\sim}{x},\underset{\sim}{n})} \, (\underset{\sim}{H} - H_n \underset{\sim}{n}) = \underset{\sim}{v}_f^{\pm} \qquad \text{(a)}$$

$$\frac{d\underset{\sim}{p}}{dt} = - (\underset{\sim}{p} \cdot \nabla) - \underset{\sim}{p} \times (\nabla \times \underset{\sim}{u}) \mp p \nabla c_f \; . \qquad \text{(b)} \qquad (3.9)$$

The upper and lower signs in the right members of these equations correspond to the "+" and "-" Hamiltonians, respectively. In equation (3.7) sgn $(\underset{\sim}{H} \cdot \underset{\sim}{p})$ denotes the sign of $\underset{\sim}{H} \cdot \underset{\sim}{p}$ and in equations (3.8) and (3.9) the quantity Q is defined by

$$Q = \left[ (1 + r)^2 - 4\, r\, (\mathbf{H} \cdot \mathbf{n})^2 / H^2 \right]^{\frac{1}{2}} ; \qquad (3.10)$$

the ratio is defined in equation (2.22). The vectors $\mathbf{v}_A^+$ ($\mathbf{v}_A^-$), $\mathbf{v}_s^+$, ($\mathbf{v}_s^-$) and $\mathbf{v}_f^+$ ($\mathbf{v}_f^-$) are called the *forward (backward) ray velocities*. Observe that in all cases

$$\mathbf{p} \cdot \frac{d\mathbf{x}}{dt} = 1, \qquad t \geq t_o \qquad (3.11)$$

where $t_o$ is regarded as the initial instant. This relation follows directly from the ray equations and the fact that $\mathbf{u} \cdot \mathbf{p} \pm p\, c_i = 1$, $i = 1,2,3$ [see equations (3.5) and (3.6)]. It should be observed that, as in crystal optics, the phase normal $\mathbf{p}$ is not in general directed along the ray.

Now let $\mathbf{x}^o = \mathbf{f}^o\,(\xi_1,\xi_2)$ be the equation, in parametric form, of any member of the family of phase fronts (see equation (2.9 ) and let[7] $\mathbf{p}^o = \mathbf{\Pi}^o(\xi_1,\xi_2)$ the wave normal at $\mathbf{x} = \mathbf{f}^o(\xi_1,\xi_2)$. Then one can in principle determine solutions of each of the above ray systems of the form

$$\mathbf{x}_i^{\pm} = \mathbf{f}_i^{\pm}\,(\xi_1,\xi_2,\, t - t_o), \qquad (3.12)$$

$$\mathbf{p}_i^{\pm} = \mathbf{\Pi}_i^{\pm}\,(\xi_1,\xi_2,\, t - t_o) \qquad (3.13)$$

such that $\mathbf{f}_i^{\pm}\,(\xi_1,\xi_2,\,0) = \mathbf{f}^o(\xi_1,\xi_2)$ and $\mathbf{\Pi}_i^{\pm}\,(\xi_1,\xi_2,\,0) = \mathbf{\Pi}_i^o(\xi_1,\xi_2)$

---

[7] Note that $\mathbf{p}^o = p^o\mathbf{n}$, where $\mathbf{n} = \mathbf{n}(\xi_1,\xi_2)$ is the unit normal to the phase front at $(\xi_1,\xi_2)$. Substituting $\mathbf{x}^o = \mathbf{f}^o(\xi_1,\xi_2)$ and $\mathbf{p}^o = p^o\mathbf{n}$ into $\mathcal{H}_i^{\pm}\,(\mathbf{x},\mathbf{p}) = 0$, $i = 1,2,3$ we obtain, in general, six values of $p^o$ thereby fixing the initial value of $\mathbf{p}$ in each of the equations (4.12) - (4.14).

for all $i$[8]. It is assumed here and in equation (3.12), that i takes on the values s, A and f. Equations (3.12) and (3.8) expresses in parametric form the six phase fronts evolving out of the initial manifold. In geometrical terms the situation may be described as follows: $\delta\mathcal{S}(t_o)$, in Figure 2, represents a small neighborhood of the point $\underset{\sim}{x}^o = \underset{\sim}{f}^o(\xi_1,\xi_2)$ on the initial phase front $\mathcal{S}(t_o)$. This elemental phase front splits up into six elemental phase fronts $\delta\mathcal{S}_i^{\pm}(t)$, $i = s, A, f$, propagating with the instantaneous velocity $\underset{\sim}{v}_i^{\pm}$, $i = s, A, f$ along their associated rays. The positions and orientations of the $\delta\mathcal{S}_i^{\pm}(t)$ at each instant of time is given by equations (3.12) and (3.13), respectively. As the parameters $\xi_1$ and $\xi_2$ range over their domain of definition $\delta\mathcal{S}(t_o)$ sweeps out the reference phase front $\mathcal{S}(t_o)$ while the $\delta\mathcal{S}_i^{\pm}(t_o)$ sweep out the six fronts $\mathcal{S}_i^{\pm}(t)$, into which $\mathcal{S}(t_o)$ has evolved.

Let $\underset{\sim}{F}_i^{\pm}$, ($i$ = s, A and f) denote the flux (see equation (2.6)) associated with a fundamental wave of type ($\pm$, i). Combining equation (2.6) with the formulas for $\delta\underset{\sim}{H}^{(0)}$, $\delta\underset{\sim}{u}^{(0)}$, $\delta\rho^{(0)}$, and simplifying the results with the aid of equation (2.18), it is found after some manipulation that

$$\underset{\sim}{F}_i^{\pm} = (\epsilon_i^{\pm})^2 \, \underset{\sim}{v}_i^{\pm}, \qquad i = s, A, f \quad . \tag{3.14}$$

In this equation[9], $(\epsilon_i^{\pm})^2$ is the energy density, measured in units of $E_i$, (see last equations of (2.24) and (2.25)) on the ($\pm$, i) - ray at time t. An explanation of how to calculate the $\epsilon_i^{\pm}$ from their initial values (see equation (2.28)) will be given in the next section. Here, we merely note that equation (3.14) is the precise form of the statement "the rays are conveyors of energy".

---

[8] Solving for $\xi_1,\xi_2$ and $t-t_o$ in terms of $x_1$, $x_2$, $x_3$ in equation (3.12) we obtain three equations one of which is of the form $t-t_o = W(\underset{\sim}{x})$. In this way way we obtain $W(\underset{\sim}{x})$.

[9] We shall henceforth append the subscript i, $i = s,A,f$ to the quantities $\underset{\sim}{F}, \epsilon$, E, etc. in order to identify the fundamental wave to which these quantities correspond.

### B. Variation of the Strengths of the Fundamental Waves along the Rays.

Let $\mathcal{S}_i^{\pm}$, $t > t_o$ denote the ($\pm$, i)-th phase front that has evolved out of the reference phase front $\mathcal{S}(t_o)$ (see equation (2.7)). Let

$$\delta\, D_i^{\pm}(\underset{\sim}{x}) \quad = \quad \epsilon_i^{\pm}(\underset{\sim}{x})\ R_i^{\pm}(\underset{\sim}{x},\underset{\sim}{n}) \tag{3.15}$$

denote the disturbance at a point $\underset{\sim}{x}$ of $\mathcal{S}_i^{\pm}(t)$. As in Section II, $\underset{\sim}{n} = \underset{\sim}{n}(\underset{\sim}{x})$ is the normal to $\mathcal{S}_i^{\pm}(t)$ at $\underset{\sim}{x}$ and $R_i^{\pm}(\underset{\sim}{x},\underset{\sim}{n})$ is the normalized eigenvector of the matrix M (equation (2.14)) associated with the disturbance speed $\pm\, c_i$. To complete the geometrical solution, it is necessary to determine the variation of $\delta D_i^{\pm}(\underset{\sim}{x})$ at each point of $\mathcal{S}_i^{\pm}(t)$ for all $t > t_o$, given that $\delta D^{\pm}(x)$ is specified on $\mathcal{S}(t_o)$ by

$$\delta D_i^{\pm}(\underset{\sim}{x})\Big|_{t\,=\,t_o} = \epsilon_{i,o}^{\pm}(x)\ R_{i,o}^{\pm}(\underset{\sim}{x},\underset{\sim}{n}), \tag{3.16}$$

(see equation (2.28)).

Now $\underset{\sim}{n} = \underset{\sim}{p}(t)/p(t)$ is known as each of the rays $\underset{\sim}{x} = \underset{\sim}{x}(t)$ used in the construction of $\mathcal{S}_i^{\pm}(t)$. Consequently, $R_i^{\pm}\,[\underset{\sim}{x}(t),\, \underset{\sim}{n}(t)]$ is known for all $t > t_o$ at each point of $\mathcal{S}_i^{\pm}(t)$. The problem therefore comes down to determining how $\epsilon_i^{\pm}\,(\underset{\sim}{x})$ varies along these rays. It can be shown[10] that $\epsilon_i^{\pm}\,[\underset{\sim}{x}(t)]$ is determined from the following equation:

---

[10] We outline a proof in Appendix I.

$$\left\{ A_i^{\pm}(\underset{\sim}{x})\, U_i^{\pm}(\underset{\sim}{x})(\epsilon_i^{\pm}(\underset{\sim}{x}))^2 \right\} \Bigg|_{\underset{\sim}{x} = \underset{\sim}{x}(t)} = \left\{ U_i^{\pm}(\underset{\sim}{x})(\epsilon_i^{\pm}(\underset{\sim}{x}))^2 \right\} \Bigg|_{\underset{\sim}{x}=\underset{\sim}{x}(t_o)} \cdot \exp\left[ \int_{t_o}^{t} T_i(t)dt \right]$$

$$i = s,\ A,\ f. \tag{3.17}$$

In this equation, $\underset{\sim}{x} = \underset{\sim}{x}(t)$ is the ray through $\underset{\sim}{x}_o = \underset{\sim}{x}(t_o)$ associated with the fundamental mode under discussion. The functions $T_i(t)$, $i =$ s, A, f are

$$T_A = \frac{1}{2} (\underset{\sim}{u} \cdot \nabla \log \rho) \Big|_{\underset{\sim}{x} = \underset{\sim}{x}(t)} \tag{3.18}$$

$$T_i = \frac{\sigma_i}{a^2 + b^2 - 4a^2\, b_n^2} \left\{ \frac{\mu}{\rho} \left[ (\underset{\sim}{H} \cdot \nabla)\underset{\sim}{u} \right] \cdot \underset{\sim}{H} - c_i^2 \left[ (\underset{\sim}{n} \cdot \nabla)\underset{\sim}{u} \right] \cdot \underset{\sim}{n} \right. \tag{3.19}$$

$$\left. + \frac{\underset{\sim}{u}}{2} \cdot \left[ (c_i^2 - a^2) \nabla \log \rho + \frac{c_i^2 - b_n^2}{c_i^2} \nabla a^2 \right] \right\} \Bigg|_{\underset{\sim}{x} = \underset{\sim}{x}(t)},$$

$$i = s,\ f$$

where

$$\sigma_i = \begin{cases} -1, & \text{if } i = s, \\ +1, & \text{if } i = f \end{cases} \tag{3.20}$$

$A_i^{\pm} [\underset{\sim}{x}(t)]$, the so-called expansion ratio along the ray, is defined as follows: Let $d\sigma_o$ denote an element of area at $\underset{\sim}{x}_o$ on $\mathcal{S}(t_o)$. Let $d\sigma_i^{\pm}$ be the differential area on $\mathcal{S}_i^{\pm}(t)$ which corresponds to $d\sigma_o$, the correspondence being effected by the tube of rays through $d\sigma_o$. Then

$$A_i^{\pm} [\underset{\sim}{x}(t)] \equiv \frac{d\sigma_i^{\pm}}{d\sigma_o}, \tag{3.21}$$

Since $U = p^{-1}$ (see equation (3.2)), U is known at all points of $\underset{\sim}{x} = \underset{\sim}{x}(t)$.

Noting that $\underset{\sim}{F}_i^{\pm} \cdot \underset{\sim}{n}_i^{\pm} = (\epsilon_i^{\pm})^2\, U_i^{\pm}$ (see equations (3.14) and (3.7) - (3.11)) and combining this fact with equation (3.17) we find that

$$A_i^{\pm}\, \underset{\sim}{F}_i^{\pm} \cdot \underset{\sim}{n}_i^{\pm} \Big|_{\underset{\sim}{x} = \underset{\sim}{x}(t)} = A_i^{\pm}\, \underset{\sim}{F}_i^{\pm} \cdot \underset{\sim}{n}_i^{\pm} \Big|_{\underset{\sim}{x} = \underset{\sim}{x}(t_o)} \exp\left[\int_{t_o}^{t} T_i(t)\, dt\right] \qquad (3.22)$$

In this form, we see that the normal of flux of wave energy out of a tube of rays intercepting the area $d\sigma_i^{\pm}$ on the phase front $\mathcal{S}_i^{\pm}(t)$ is proportional to the influx of wave energy through $d\sigma_o$. The proportionality factor $\exp\left[\int_{t_o}^{t} T_i(t)\, dt\right]$ has its origin in coupling of the fundamental disturbance waves to the underlying motion of the medium which supplies energy to the tube. In the important special cases where $\underset{\sim}{u} \equiv 0$, and where both $\rho$ and $\underset{\sim}{u}$ are constant, $T_i(t) \equiv 0$ in all of the fundamental waves, and equation (3.17) reduces to

$$A_i^{\pm}[\underset{\sim}{x}(t)]\; c_i\,[\underset{\sim}{x}(t), \underset{\sim}{n}(t)]\; (\epsilon_i^{\pm}[\underset{\sim}{x}(t)])^2 = c(\underset{\sim}{x}_o, \underset{\sim}{n}_o)(\epsilon_{i,o}^{\pm})^2 \qquad (3.23)$$

This result is true whether $\underset{\sim}{H}$ is constant or not. If in addition, $\underset{\sim}{H}$ is constant, then the rays are straight lines, (see Section C below), $U\,[\underset{\sim}{x}(t)] = p^{-1}(t)$ is constant along $\underset{\sim}{x} = \underset{\sim}{x}(t)$, and equation (3.23) reduces to

$$A_i^{\pm}[\underset{\sim}{x}(t)]\; (\epsilon_i^{\pm}[\underset{\sim}{x}(t)])^2 = (\epsilon_{i,o}^{\pm})^2 \qquad i = s, A, f\,. \qquad (3.24)$$

In this case, it follows from the theory of surfaces that

$$A_i^{\pm}[\underset{\sim}{x}(t)] = \frac{K_o\,[\underset{\sim}{x}(t_o)]}{K_i^{\pm}[\underset{\sim}{x}(t)]} \qquad (3.25)$$

In this equation, $K_o\,[\underset{\sim}{x}(t_o)]$ and $K_i^{\pm}[\underset{\sim}{x}(t)]$ denote the Gaussian curvatures at $\underset{\sim}{x}(t_o)$ and $\underset{\sim}{x}(t)$ of the phase fronts $\mathcal{S}(t_o)$ and $\mathcal{S}_i^{\pm}(t)$ both of which are assumed to have curvature at these points.

Very little of the discussion in this or in the preceding sections requires modification when gravitational effects are included. Specifically, the addition of the "gravitational" terms $\rho \nabla \Phi$ and $\delta\rho\nabla\Phi$ to the appropriate members of equations (2.1) $\underset{\sim}{A}_2$ and (2.2)$\delta$ $\underset{\sim}{A}_2$ respectively is found to have no effect on the formulas[11] for the disturbance speeds, fundamental waves, wave energies and wave fluxes. The presence of the gravitational terms is felt only in the expressions for the $T_i$, $i = s, A, f$ given above and then only in the addition of the term

$$T_{i,\, grav} = \frac{-\,c_i}{c_i^4 - a^2\, b_n^2} \left[ b_n^2 \, \frac{\underset{\sim}{H}}{H_n} - c_i^2 \, \underset{\sim}{n} \right] \cdot \nabla \Phi, \qquad i = s, f \;. \quad (3.26)$$

to $T_i$ in the case of slow and fast waves. $T_A$ requires no change whatsoever.

## C. Geometrical Construction of the Phase Fronts

### Huygens' Construction

Again let $\delta\mathcal{S}(t_o)$ be a small neighborhood of the point $\underset{\sim}{x}_o$ with normal $\underset{\sim}{n}_o = \underset{\sim}{n}(\underset{\sim}{x}_o)$ on the reference phase front. Suppose $\rho$, $\underset{\sim}{H}$ and $\underset{\sim}{u}$ are everywhere constant. Then it follows immediately from equation (3.7) - (3.9) that on each ray through $\underset{\sim}{x}_o$, $\underset{\sim}{n} = \underset{\sim}{p}(t)/p(t)$ is a constant and is equal to $+\underset{\sim}{n}_o$ or $-\underset{\sim}{n}_o$ according as the ray is a forward or backward ray. Furthermore, each of the six rays through $\underset{\sim}{x}_o$ is a straight line. The

---

[11] The formulas mentioned here do not depend explicitly on $\Phi$. However, the parameters r and b appearing in these formulas are of course affected by the presence of $\Phi$.

$\delta \mathcal{S}_i^{\pm}(t)$, $i = s, A, f$ are thus carried parallel to themselves along their rays. Explicit formulas can be given for the phase fronts evolving out of $\mathcal{S}(t_0)$ as soon as the equation for $\mathcal{S}(t_0)$, $\underset{\sim}{x}_0 = f^0(\xi_1, \xi_2)$ is specified[12]. Here, we shall limit ourselves to constructing these phase fronts by purely geometrical means. For the sake of simplicity it will be assumed that $\underset{\sim}{u}$ vanishes everywhere.

In Figure 3 we show the position of $\delta\mathcal{S}_f^{+}$ at time $t > t_0$. Now according to equations (3.3) and (3.11)

$$\underset{\sim}{n} \cdot \frac{d\underset{\sim}{x}}{dt} = \underset{\sim}{n}_0 \cdot \frac{d\underset{\sim}{x}}{dt} = \frac{1}{p(t)} = c[\underset{\sim}{x}(t), \underset{\sim}{n}\,(x(t)] \tag{3.27}$$

on all rays. Since $\underset{\sim}{H}$ and $\rho$ are constant we conclude that

$$\underset{\sim}{n} \cdot \frac{d\underset{\sim}{x}}{dt} = c\,(\underset{\sim}{n}_0) = \text{const.}, \tag{3.28}$$

so that, in particular, for the fast forward ray

$$\underset{\sim}{n} \cdot \frac{d\underset{\sim}{x}}{dt} = c_f\,(\underset{\sim}{n}_0) = \text{const.} \tag{3.29}$$

The vector

$$\overrightarrow{P_0F} = c_f\,(\underset{\sim}{n}_0)(t - t_0)\,\underset{\sim}{n}_0 \tag{3.30}$$

therefore gives the displacement of $\delta\mathcal{S}_f^{+}$ along the direction $\underset{\sim}{n}_0$ and the plane $\mathcal{T}(F)$ drawn perpendicular to $\overrightarrow{P_0F}(P_0)$ at $F(P_0)$ is therefore tangent to $\delta\mathcal{S}_f^{+}(t)$ at the point $P$ ($\underset{\sim}{x} = \underset{\sim}{x}(t)$). This fact suggests the following construction. At each point $P_0$ of $\mathcal{S}(t_0)$ draw the vector $\overrightarrow{P_0F}(P_0) = c_f(\underset{\sim}{n}_0)(t - t_0)\underset{\sim}{n}_0$. Next pass a plane $\mathcal{T}[F(P_0)]$ through $F(P_0)$

---

[12] The phase fronts evolving out of an initially spherical phase front are described in [1b].

which is normal to the vector $\overrightarrow{P_oF}(P_o)$. Then clearly the envelope of these planes is $\mathcal{S}_f^+(t)$. It need hardly be said that the remaining phase fronts may be constructed in an analogous manner.

Suppose in particular that $\mathcal{S}(t_o)$ is a "small" sphere of radius $\epsilon$ located at the origin of coordinates. By "small" we mean that $\epsilon$ is negligible compared with the distances travelled in one second by the $\mathcal{S}_i^{\pm}(t)$ evolving out of $\mathcal{S}(t_o)$. For the sake of definiteness let $\underset{\sim}{H}$ be taken along the x-axis and assume that the ratio $r = a^2/b^2$ is .5. The x-axis is evidently an axis of revolution so that it is enough to consider the cross section in the (x,y)-plane. Such a cross section is shown in Figure 4. The $\mathcal{S}_s^{\pm}$-curves are the two cusped figures. The $\mathcal{S}_A^{\pm}$-curves are two points (actually two spheres of radius $\epsilon$) located at $\pm$ b; in this type of wave motion $\mathcal{S}(t_o)$ splits up into two spheres congruent to $\mathcal{S}(t_o)$ which propagate along the $\underset{\sim}{H}$-direction, with velocities $\pm$ b. The $\mathcal{S}_f^{\pm}$-curves are shown as one oval-like curve. They are actually of the order of $\epsilon$ apart. Figure 5 shows why this is the case. Assuming the outward normals to $\mathcal{S}_o(t)$ correspond to the forward propagating waves, we see the $\mathcal{S}_f^-$ portion of the wave front comes from diametrically opposite points on the sphere.

The curves of Figure 4 are typical of those associated with values of r in the range $r < 1$. In the range $r > 1$, the Alfven circles are tangent to the $\mathcal{S}_s^{\pm}$ curves on the $\underset{\sim}{H}$-axis but the general appearance of the curves remain the same. The case $r = 1$ is somewhat special; it is discussed in detail in reference [1b].

Since we have drawn Figure 4 as if $\epsilon$ were zero, we may think of the phase fronts pictured there as emerging from a point source. These phase fronts correspond in crystal optics to Fresnel's ray surface. We refer to them here as *Friedrich's ray surfaces*[12] or simply as *spheres* or *wavelets* and henceforth denote by $\mathcal{F}_i^{\pm}(t,P_o)$, i = s, A, f the wavelets (at time t) that have issued from the point $P_o$ at time $t_o < t$.[13]

As in acoustics and geometrical optics, one may employ these spheres to obtain an alternative construction of the phase fronts that evolve out of $\mathcal{S}(t_o)$. This construction, known as *Huygens' construction*, consists in drawing the spheres $\mathcal{F}_i^{\pm}(t,P_o)$ at each point $P_o$ of $\mathcal{S}(t_o)$ and then forming the envelopes. The justification of this method is to be found in our previous discussion. Consider, for example, the construction of $\mathcal{S}_f^+(t)$ which was explained in reference to Figure 3. Imagine superimposed on this diagram the sphere $\mathcal{F}_f^+(t,P_o)$ centered at $P_o$ on $\delta\mathcal{S}(t_o)$ where, as indicated, the normal is $n_o$. Consider the ray on $\mathcal{S}^+(t,P_o)$ whose projection on $n_o$ is $c_f(n_o)(t - t_o)n$. Recalling the way $\mathcal{F}_f^+(t,P_o)$ was constructed, one readily verifies that this ray coincides to $\overrightarrow{P_oP}$ of the figure and that $\mathcal{F}_f^+(t,P_o)$ is tangent to $\mathcal{S}_f^+(t)$ at P. From these remarks, it follows immediately that the envelope of the spheres coincides with the phase front $\mathcal{S}_f^+(t)$.

We saw in Sections A and B that the (unique) ray through $P_o$ corresponding to the normal $n_o$ to $\delta\mathcal{S}(t_o)$ at $P_o$ (see Figure 3) is the conveyor of the energy of the associated fundamental wave. In view of the above discussion the following fact is apparent. Only those rays of the spheres $\mathcal{J}_i^{\pm}(t,P_o)$ employed in Huygens' construction carry energy whose end points coincide with the points of the envelope of the spheres $\mathcal{J}_i^{\pm}(t,P^o)$. In Figure 3, $\overrightarrow{P_oP}$ is one such energy-carrying ray. The remaining fast rays issuing from $P_o$ (not shown in the figure) carry no energy; but, of course they help in the visualization of the envelope.

---

[12] They were first described by K. O. Friedrichs in [12].

[13] As explained above $\mathcal{S}_f^+(t,P_o)$ and $\mathcal{S}_f^-(t,P_o)$ coincide.

The constructions that have been described in this section are valid even if $\underset{\sim}{H}$, $\rho$ and $\underset{\sim}{u}$ are variable, provided sufficiently small time intervals are chosen. For, the basis of all constructions is the relation $\underset{\sim}{p} \cdot \frac{d\underset{\sim}{x}}{dt} = 1$ which is valid whether $\underset{\sim}{H}$, $\rho$, and $\underset{\sim}{u}$ are constant or not. To construct a phase front at time t given its position at time $t_o$, it is necessary to divide the time interval $(t_o,t)$ into small subintervals and starting with the first to carry out the foregoing constructions for each time interval in succession.

### D. Fermat's Principle

The ray equations (3.7a)-(3.9a) all have the form

$$\frac{d\underset{\sim}{x}}{dt} = \dot{\underset{\sim}{x}} = \nabla_p \mathcal{H}_i^{\pm}(\underset{\sim}{x},\underset{\sim}{p}), \qquad i = s,\ A,\ f \tag{3.31}$$

where $\nabla_p$ is the gradient in $\underset{\sim}{p}$-space. Let

$$\underset{\sim}{p} = \underset{\sim}{p}(\dot{\underset{\sim}{x}}, \underset{\sim}{x}) \tag{3.32}$$

be the solution of this equation for the components of $\underset{\sim}{p}$ in terms of the components of $\underset{\sim}{x}$ and $\dot{\underset{\sim}{x}}$. We next introduce the functions

$$\mathcal{L}_i^{\pm}(\dot{\underset{\sim}{x}},\underset{\sim}{x}) \equiv \mathcal{H}_i^{\pm}(\underset{\sim}{x}, \underset{\sim}{p}(\dot{\underset{\sim}{x}}, \underset{\sim}{x})) \tag{3.33}$$

and define the speeds $\overset{\pm}{V}_i$ as the solutions of the equations

$$\overset{\pm}{\mathcal{L}}_i \left[ \overset{\pm}{V}_i \frac{\dot{\underset{\sim}{x}}}{|\dot{\underset{\sim}{x}}|} , \underset{\sim}{x} \right] = 0, \qquad i = s, A, f \tag{3.35}$$

$\overset{\pm}{V}_i$ can be shown to be equal to the magnitude of the ($\pm$, i)-th ray velocity. More important here is the fact that $\overset{\pm}{V}_i = \overset{\pm}{V}(\dot{\underset{\sim}{x}}, \underset{\sim}{x})$ is, by definition, a homogeneous function of the degree zero in the components of $\dot{\underset{\sim}{x}}$. It follows that a change of parameter leaves the functional form of $\overset{\pm}{V}_i$ unchanged if by $\dot{\underset{\sim}{x}}$ we always understand the derivative with respect to the parameter.

An ($\pm$, i)-ray may now be characterized as the curve which makes the time of travel

$$\overset{\pm}{T}_i(\underset{\sim}{x}_o, \underset{\sim}{x}_1) = \int_{s_o}^{s_1} \frac{ds}{\overset{\pm}{V}_i(\dot{\underset{\sim}{x}}, \underset{\sim}{x})} \tag{3.36}$$

an extremum. All competing curves in this variational principle are required to pass through the points $\underset{\sim}{x}_o$ and $\underset{\sim}{x}_1$ when $s = s_o$ and $s_1$ respectively; the curve parameter s is the arc length. This is Fermat's principle. We refer the reader to R. K. Luneberg's notes [4] for the proof of this principle and a discussion of its relation to other methods of characterizing the rays. Here, we merely note that the application of Fermat's principle is limited in practice to those cases where it is easy to express $\underset{\sim}{p}$ in terms of $\underset{\sim}{x}$ and $\dot{\underset{\sim}{x}}$ and to find the roots of equation (3.35).

## IV. PROPAGATION OF ALFVEN AND FAST FRONTS IN INHOMOGENEOUS MEDIA

### A. General Remarks

To illustrate the theory of Sections II and III, we consider the propagation of Alfven phase fronts in a stationary but inhomogeneous medium. In this case, the ray and $\overset{\pm}{\epsilon}_A$-strength equations can be written in the form [see equations (3.7) and (3.23)]

$$\frac{d\underset{\sim}{x}}{d\tau} = \pm \frac{\underset{\sim}{H}}{N} \equiv \overset{\pm}{\hat{v}}_A , \tag{4.1}$$

$$(\overset{\pm}{\epsilon}_A)^2 \overset{\pm}{A}_A c_A \Big|_{\underset{\sim}{x} = \underset{\sim}{x}(\tau)} = (\overset{\pm}{\epsilon}_A)^2 c_A \Big|_{\underset{\sim}{x} = \underset{\sim}{x}(\tau_o)} . \tag{4.2}$$

Here, N is any conveniently chosen normalization constant, and the new parameter $\tau$ is defined by the equation

$$t - t_o = \frac{N}{\sqrt{\mu}} \int_{\tau_o}^{\tau} \sqrt{\rho\,[\underset{\sim}{x}(\tau')]}\; d\tau' . \tag{4.3}$$

$\overset{\pm}{A}_A$, it will be recalled, is the ratio $d\overset{\pm}{\sigma}_A/d\sigma_o$ of the areas $d\overset{\pm}{\sigma}_A(\tau)$ and $d\sigma_o = d\sigma(\tau_o)$ on the phase fronts $\overset{\pm}{\mathcal{S}}_A(\tau)$ and $\mathcal{S}(\tau_o)$, respectively, cut out by a tube of rays through $d\sigma_o$.

According to equation (4.2), $\epsilon^+(\epsilon^-)$ depends both on $\overset{+}{A}_A(A^-_A)$ and on the direction of the wavefront normal $\underset{\sim}{n}$ (since $c_A = (\mu H_n^2 \rho^{-1})^{\frac{1}{2}}$). Thus, it appears that the determination of $\overset{\pm}{\epsilon}$ requires not only the solution of (4.1) but also of the system (3.9b). However, it can be shown that

$$\frac{d\,\overset{\pm}{\sigma}_A}{d\,\sigma_o}\; c_A\, \rho^{\frac{1}{2}} \Big|_{\underset{\sim}{x} = \underset{\sim}{x}(\tau)} = c_A \rho^{\frac{1}{2}} \Big|_{\underset{\sim}{x} = \underset{\sim}{x}(\tau_o)} \tag{4.4}$$

so that equation (4.2) reduces to the surprisingly simple relation

$$(\epsilon^{\pm})^2 \rho^{\frac{1}{2}} \Big|_{\underset{\sim}{x} = \underset{\sim}{x}(\tau)} = (\epsilon^{\pm})^2 \rho^{\frac{1}{2}} \Big|_{\underset{\sim}{x} = \underset{\sim}{x}(\tau_o)} \quad . \qquad (4.5)$$

Thus the $\epsilon^{\pm}$ actually depends only on the local density and are independent of the expansion ratio. Moreover, if $\rho$ is everywhere constant, $\epsilon^{+}$ and $\epsilon^{-}$ remain constant along their rays.

To prove equation (4.5), we integrate $\nabla \cdot \hat{\underset{\sim}{v}}^{\pm}$ over the volume $\Delta V^{\pm}$ of the tube of rays between $d\sigma^{\pm}(\tau)$ and $d\sigma^{\pm}(\tau + \Delta\tau)$. Next, we employ the divergence theorem, divide both sides by $\Delta V^{\pm}$ and make use of the relations $\hat{\underset{\sim}{v}}_A^{\pm} = \underset{\sim}{v}_A^{\pm} dt/d\tau$, $\underset{\sim}{v}_A^{\pm} \cdot \underset{\sim}{n} = U_A^{\pm}$ [see equations (4.1), (3.11) and (4.3)]. Letting $\Delta\tau$ approach zero, we find that (cf. [4] p. 87).

$$\nabla \cdot \hat{\underset{\sim}{v}}_A^{\pm} = \frac{d}{d\tau} \log \left[ \frac{d\sigma_A}{d\sigma_o} \frac{U_A^{\pm}}{U_{A,o}^{\pm}} \left( \frac{\rho}{\rho_o} \right)^{\frac{1}{2}} \right] \qquad (4.6)$$

Here $\rho_o$ and $U_{A,o}$ denote the density and normal speed on $\mathcal{S}(\tau_o)$. It may be remarked that this result is completely general; $\underset{\sim}{u}$ need not vanish. In addition, it applies, with obvious change of notation, to slow and fast waves. Equation (4.4) now follows from the fact that $\nabla \cdot \hat{\underset{\sim}{v}}_A^{\pm} = \pm N^{-1} \nabla \cdot \underset{\sim}{H} = 0$.

### B. Propagation of Alfven Fronts in a Dipole Field

We turn now to the problem of determining the propagation of Alfven fronts in a dipole field. In this case, the basic equations are:

$$\underset{\sim}{H} = - \nabla \left(M \cos \theta / R^2\right), \tag{4.7}$$

$$\frac{dR}{d\tau} = - 2 \frac{M \cos \theta}{N \; R^3} , \tag{4.8}$$

$$\frac{R \, d\theta}{d\tau} = - \frac{M \sin \theta}{N R^3} , \tag{4.9}$$

$$\mathcal{S}(\tau_o): \qquad R_o = f\,(\theta_o, \phi_o) \tag{4.10}$$

Here, M is the magnetic moment of the dipole, R is the distance from the origin and $\theta$ is the polar angle measured from the vertical dipole axis. Equation (4.10) is the equation of the reference surface in polar coordinates $\phi_o$ being the azmuthal angle. For the sake of simplicity, we consider only the rays anti-parallelto the field - i.e. those which are directed into the north magnetic pole.

Eliminating $\tau$ between equations (4.8) and (4.9), we find the equation,

$$R = k_o \sin^2 \theta, \tag{4.11}$$

$$k_o = \frac{R_o}{\sin^2 \theta_o} = \frac{f\,(\theta_o, \phi_o)}{\sin^2 \theta_o} \tag{4.12}$$

for the ray through the point $(R_o, \theta_o, \phi_o)$ on $\mathcal{S}(\tau_o)$.

We now use equation (4.11) to eliminate $\theta$ in equation (4.8). On integrating, we obtain the result

$$\tau - \tau_o = \frac{N}{2M} \int_{R_o}^{R} (\mp) \frac{r^3 dr}{\sqrt{1 - (r/k_o)}} = \frac{k_o^4 N}{2\,M} \int_{R_o/k_o}^{R/k_o} (\mp) \frac{x^3}{\sqrt{1-x}}\, dx \, . \tag{4.13}$$

The minus sign in the last member is to be applied over that range of R in which $0 < 0 < \pi/2$ and the plus sign in the $\theta$-range $\pi/2 < \theta < \pi$. Setting

$$I = \frac{1}{B} \int_{o}^{x} \frac{x^3 \, dx}{\sqrt{1 - x}} , \tag{4.14}$$

where (see reference [24])

$$B = \int_{o}^{1} \frac{x^3 \, dx}{\sqrt{1 - x}} = .91428 \tag{4.15}$$

and

$$N = 2M/B, \tag{4.16}$$

we find that equation (4.13) reduces to

$$\tau - \tau_o = k_o^4 \left[ I\,(R/k_o) - I(R_o/k_o) \right] , \tag{4.17}$$

where, in virtue of equation (4.3),

$$t - t_o = \frac{2\,M}{B\sqrt{\mu}} \int_{\tau_o}^{\tau} \sqrt{\rho\,[(\tau')]} \, d\tau' . \tag{4.18}$$

I(x) will be recognized as an incomplete gamma function. Since these functions have been tabulated (see, for example, reference [24]) equations (4.17) and (4.18) furnish the solution to our problem.

For simplicity, suppose now that $\mathcal{S}(\tau_o)$ is the plane whose equation is

$$R_o = d/(\sin\theta_o \cos\phi_o) , \tag{4.19}$$

d being the distance from the dipole in the equatorial plane. If, in addition, we assume that $\rho$ is everywhere constant then

$$t - t_o = \frac{2M}{B} (\tau - \tau_o), \tag{4.20}$$

and $\tau$ is proportional to t. In Figure 6, we have pictured the evolution of the phase fronts in the meridianal plane $\phi_o = 0$ from the "time" $\tau_o = 0$ onward. The normal $\underset{\sim}{n}_o$ to $\mathcal{S}(0)$ is assumed to point to the left and to define the forward direction. The curves shown correspond to the $\tau$-values 0, .1, .2, .3 and .4. To keep the diagram uncluttered, we show $\mathcal{S}^+_A(\tau)$ on the upper half of the diagram and $\mathcal{S}^-_A(\tau)$ on the lower half. The complete picture is obtained by adding to the curves already present their reflections in the (x/d)-axis. Since the rays associated with the Alfven mode are the field lines and since these lines converge at the origin, one might expect the phase front to develop a sharp peak as it nears the dipole. We see from the figure that this is indeed the case. The dashed line is the field line on which the peak develops. Its equation, obtained from the figure, is

$$R \cong 1.154 \sin^2 \theta. \tag{4.21}$$

It may be imagined that the formation of the peak corresponds to a concentration of energy at the peak. However, this is not the case, since according to equation (4.5) the disturbance strength remains constant along a ray.

We have already established the close relationship between the time harmonic theory and the pulse theory. This relationship allows as to regard to the $\mathcal{S}(0)$ in Figure 6 either as an initial surface of discontinuity or as a fixed surface in space carrying a disturbance whose strength varies harmonically in time. In either case, if Figure 6 is to make sense, it must be assumed that the disturbance at $\mathcal{S}(0)$ is of the form $\epsilon^{+}_{A,0}\ R^{+}_{A,0} + \epsilon^{-}_{A,0}\ R^{-}_{A,0}$ (see equations (2.28)) and that $\epsilon^{\pm}_{A,0} \neq 0$. If for example $\epsilon^{-}_{A,0}$ then the backward propagating front $\mathcal{S}^{-}_{A}(\tau)$ must be ignored since it carries no disturbance.

An "earth" of radius $\alpha$ d, $0 \leq \alpha \leq 1$, can be indicated on Figure 6 by drawing a circle of radius $\alpha$ d centered at the origin. The semicircle C in Figure 6 corresponds to an earth of radius 1/5 d. Let us for the moment regard $\mathcal{S}(0)$ as a surface of discontinuity. Then $\mathcal{S}^{+}_{A}(\tau)$ and $\mathcal{S}^{-}_{A}(\tau)$ are Alfven discontinuity fronts. The figure indicates that $\mathcal{S}^{+}_{A}(\tau)$ reaches the earth first at the point P where the peak just makes contact with C. Then the disturbance spreads over higher and lower latitudes as the front behind the peak passes over C. (We are ignoring here the effect of the earth on the disturbance wave). If we imagine that the region to the left of $\mathcal{S}(0)$ is undisturbed while the region to the right is disturbed then we may safely conjecture that the disturbance at each latitude will undergo two rapid changes. At P, for example, the first change occurs when the peak reaches the earth and the second when the disturbance on the surface element located at P' has reached P after traversing the dashed field line in the counterclockwise direction.

### C. Propagation of Fast Waves in the Earth's Magnetosphere

In the earth's magnetosphere, the sound speed is much less than the Alfven speed. For this reason, we may ignore all but the first terms in expansions involving the parameter $r = a^2/b^2$. We then find that the slow disturbance speed vanishes and that the fast disturbance speed and fast ray equations reduce to

$$c_f = (\mu H^2 \rho^{-1})^{\frac{1}{2}} \equiv b, \tag{4.22}$$

$$\frac{d\underset{\sim}{x}}{dt} = b^2 \underset{\sim}{p} = b\,\underset{\sim}{n}, \tag{4.23}$$

$$\frac{d\underset{\sim}{p}}{dt} = -\, p \nabla b\ . \tag{4.24}$$

Here, we have used the fact that $p = c_f^{-1}$.

For simplicity, we henceforth limit the analysis to magnetic fields whose magnitude may be expressed in the form $|\underset{\sim}{H}| = \text{const.}\ R^{-n}$, where $R = \sqrt{x^2 + y^2}$. This choice allows us to represent a uniform field ($n = 0$), the field of a line current ($n = 1$), a two-dimensional dipole ($n = 2$) and the field in the equatorial plane of a three dimensional dipole ($n = 3$). Note that any two-dimensional multipole field has the desired form. This follows the fact that the complex conjugate $H^* = H_x - iH_y$ of such a field has the form $H^* = A\, z^{-n}$, $z = x + iy$, from which it follows that $H^2 = H^* H = |A|^2 R^{-2n}$.

Eliminating $\underset{\sim}{p}$ between equations (4.23) and (4.24), we find that

$$\frac{d}{dt}\left(\frac{1}{b^2}\,\frac{d\underset{\sim}{x}}{dt}\right) = 2 \nabla b^{-2}\ . \tag{4.25}$$

Introducing the polar coordinates $(R, \phi)$ and assuming that the density depends solely on $R$, we conclude from this equation that

$$\frac{R^2}{b^2}\,\dot{\phi} = \frac{R_o^2\,\dot{\phi}_o}{b_o^2} \equiv L\,(R_o, \phi_o; \underset{\sim}{n}_o)\,, \tag{4.26}$$

where the initial value $\dot{\phi}_o$ is to calculated from equation (4.23). Next, we dot equation (4.23) with itself and and find that

$$\dot{R}^2 + R^2\,\dot{\phi} = b^2. \tag{4.27}$$

The last two equations lead directly to the differential equations

$$\frac{d\,t}{d\,R} = \frac{\rho^{\frac{1}{2}}\,R^{2n+1}}{\alpha\sqrt{R^{2n+2} - \alpha^2 L_o\,\rho^{-1}}}\,, \tag{4.28}$$

$$\frac{d\,\phi}{d\,R} = \frac{\alpha\,L_o\rho^{\frac{1}{2}}}{\sqrt{R^{2n+2} - \alpha^2 L_o^2\,\rho^{-1}}}\,. \tag{4.29}$$

Here, we have made use of the fact that

$$b = \alpha\,\rho^{-\frac{1}{2}}R^{-n}\,, \tag{4.30}$$

$\alpha$ being same positive constant. When $\rho$ is everywhere constant we obtain the explicit results

$$t - t_o = \frac{\sqrt{\rho}}{(n+1)\alpha}\left\{\sqrt{R^{2n+2} - L_o^2\,\alpha^2\,\rho^{-1}} - \sqrt{R_o^{2n+2} - L_o^2\,\alpha^2\,\rho^{-1}}\right\} \tag{4.31}$$

$$R^{n+1} \cos \left[(n+1)(\phi + \beta)\right] = \alpha L_o / \sqrt{\rho} \qquad (4.32)$$

In equation (4.32) $\beta$ is a constant of integration which is determined by evaluating the left member of $(R_o, \phi_o)$ on the phase front.

In the magnetosphere $\rho$ is a complicated function of R and numerical integration is necessary. Employing the density profile in the magnetoshere W. E. Frances et al. [25] have calculated several ray paths in the equatorial plane issuing from a point source. These authors obtain their ray equations by postulating Fermat's principle using b (see equations (4.22) and (3.36)) as the ray speed. It would be worthwhile to extend these calculations, now that they have been placed in their proper context, to derive the strengths and form of the fronts that originate in suitable extended sources. It is our intention to investigate this question in a future report.

# V. THE LAWS OF REFLECTION AND REFRACTION

## A. Preliminary Remarks. Snell's Laws

It has thus far been assumed that the undisturbed medium is everywhere continuous. Suppose now that a surface of discontinuity $\mathcal{D}$ separates two different states of the undisturbed medium. For the sake of simplicity, we shall require $\mathcal{D}$ to be fixed in space although our results apply, with obvious modifications, to the case where $\mathcal{D}$ is in motion and changes shape. Imagine that one of the three fundamental disturbance waves is incident on $\mathcal{D}$. Denote by $\mathcal{W}_i$, the incident phase front, where i = s, A, f, and suppose that the position of $\mathcal{W}_i$ and the disturbance strength at each point of $\mathcal{W}_i$ are known at the reference time $t_o$. The basic problems of the theory are then to determine (1) the laws of reflection and refraction and the motion of the scattered phase fronts, (2) the strengths of the scattered waves in terms of the strength of the incident wave.

We shall be concerned here with the first of these problems. Formulas for the strength of the scattered waves emerging from various discontinuities are given in references [1] [22] and [23].

Unless otherwise mentioned, it is assumed that the state of the unperturbed medium on each side of the surface of discontinuity $\mathcal{D}$ is constant and that the incident phase fronts are planar. It should therefore be stressed that all results obtained for this special case apply locally (in the neighborhood of the curve of intersection of $\mathcal{D}$ with the incident front $\mathcal{W}_i$) when $\mathcal{D}$ or the incident wave is curved or when the undisturbed media separated by $\mathcal{D}$ are non-uniform.

Figures 7 and 8 depict the basic geometrical set up. $\mathcal{D}$ represents the surface of discontinuity separating the upper half-space $\mathcal{R}'$ from the lower half-space $\mathcal{R}$. The vector $\underset{\sim}{H}$ is the prevailing magnetic field at the origin 0. The local plane of incidence at the origin 0, determined by the normal on the incoming wave front and the unit normal $\underset{\sim}{N}$ on $\mathcal{D}$ at 0, is assumed to coincide with the (x,z)-plane and is denoted by $I_I$. As shown, $\underset{\sim}{N}$ is directed along the positive z-axis. The vector $\underset{\sim}{H}_I$ is the projection of $\underset{\sim}{H}$ on the plane of incidence. The quantities $\psi_H$, $0 \leq \psi_H \leq \pi/2$ and $\theta_H$, $-\pi < \theta_H < \pi$, are the angles between $\underset{\sim}{H}$ and $\underset{\sim}{H}_I$ and $\underset{\sim}{H}_I$ and $\underset{\sim}{N}$, respectively. We shall have occasion to refer to the angles $\beta$ and $\gamma$ of Figure 7 later.

In the above remarks and in the drawing of Figure 7, it has been implicitly assumed that $\underset{\sim}{H}$ is continuous across $\mathcal{D}$. This need not be the case; $\mathcal{D}$ may, for example, be a stationary hydromagnetic shock. Accordingly, we shall write $\underset{\sim}{H}$ for the magnetic intensity in $\mathcal{R}$ and use $\underset{\sim}{H}'$ to denote this quantity in $\mathcal{R}'$. In general, if Q is any quantity in $\mathcal{R}$, we employ Q' to denote the corresponding quantity in $\mathcal{R}'$ whenever $Q \neq Q'$.

Figure 8(a) shows the phase fronts in the plane of incidence. $\mathcal{W}_i$ denotes the incoming phase front, propagating toward $\mathcal{D}$ from below. We take $\mathcal{W}_i$ to be fast, Alfven or slow according as i = 1, 2, or 3. $\mathcal{W}_{i1}$, $\mathcal{W}_{i2}$ and $\mathcal{W}_{i3}$ denote, in the order stated, the reflected fast, Alfven and slow phase fronts and $\mathcal{W}_{i4}$, $\mathcal{W}_{i5}$ and $\mathcal{W}_{i6}$ the refracted slow, Alfven and fast phase fronts - all produced by the incident wave of type (i). Figure 8(b) shows the disposition of the normals $\underset{\sim}{n}_i$ and $\underset{\sim}{n}_{ij}$ on these wave fronts; to keep the diagram uncluttered only three normals have actually been drawn. The normals point along the direction of propagation of their fronts (see equations (2.9) and (2.11)). The angle $\theta_i$, $-\pi/2 \leq \theta_i \leq \pi/2$, is the angle between $\underset{\sim}{N}$ and the incident phase normal $\underset{\sim}{n}_i$. Here, and in the following, angles in the plane of incidence are regarded positive or negative according as their sense is clockwise or counterclockwise. We accept at this point the easily established fact [22] that the phase normals $\underset{\sim}{n}_{ij}$ of the scattered waves all lie in the plane of incidence. Then we denote by $\theta_{ij}$, $j = 1, \ldots, 6$, angles (in the plane of incidence) between $\underset{\sim}{N}$ and the j-th scattered wave. Specifically, when $j = 1,2$ or $3$, the angle $\theta_{ij}$, $-\frac{\pi}{2} \leq \theta_{ij} \leq \frac{\pi}{2}$, is the angle between $\underset{\sim}{N}$ and the j-th reflected wave. When $j = 4, 5$, or $6$, $\theta_{ij}$ is the angle between $\underset{\sim}{N}$ and the j-th transmitted wave.

In the plane at incidence I (see Figure 7) the incident and scattered phase fronts intersect in a common point 0 which, it will be supposed, moves with the velocity $\underset{\sim}{V} = V \underset{\sim}{x}_0$ at the instant depicted. $\underset{\sim}{V}$ is called the trace velocity. Let $U_i > 0$ be the speed at 0 in the normal direction $\underset{\sim}{n}_i$ (see equation (2.10)) of the incident phase front and let $U_{ij}$ denote the corresponding normal speeds of the scattered waves. From the fact that $\mathcal{W}_i$ and the $\mathcal{W}_{ij}$ intersect at 0 and move together with common velocity $\underset{\sim}{V}$, we conclude immediately that for any i, $i = 1,2,3$, that

$$\underset{\sim}{V} \cdot \underset{\sim}{n}_i = U_i, \tag{5.1}$$

and

$$\underset{\sim}{V} \cdot \underset{\sim}{n}_{ij} = U_{ij} \qquad j = 1,2,\ldots,6. \tag{5.2}$$

We have seen that normal speeds are direction-dependent. This dependence on direction is made explicit in the following manner:

$$U_i = \underset{\sim}{u}_I \cdot \underset{\sim}{n}_i \pm c_i \qquad i = 1, 2, 3, \tag{5.3}$$

where

$$\frac{c_1}{b} = \left\{ \frac{1+r}{2} + \frac{1}{2}\left[(1+r)^2 - 4r\cos^2\psi_H \cos^2(\theta_1-\theta_H)\right]^{\frac{1}{2}} \right\}^{\frac{1}{2}}, \tag{5.4}$$

$$\frac{c_2}{b} = \cos\psi_H \left|\cos(\theta_2 - \theta_H)\right| , \tag{5.5}$$

$$\frac{c_3}{b} = \left\{ \frac{1+r}{2} - \frac{1}{2}\left[(1+r)^2 - 4r\cos^2\psi_H \cos^2(\theta\ -\theta_H)\right]^{\frac{1}{2}} \right\}^{\frac{1}{2}} \tag{5.6}$$

In equation (5.3), $\underset{\sim}{u}_I$ is the projection of $\underset{\sim}{u}$ on the plane of incidence. The quantities $c_1$, $c_2$ and $c_3$ are, in the order stated, the slow, Alfven and fast disturbance speeds. The quantity r, it will be recalled, is the squared ratio $a^2/b^2$ of the sound speed a to the Alfven disturbance speed $b = \sqrt{\mu H^2 \rho^{-1}}$. Equation (5.3) follows directly from the definition of $U_i$ (see equation (2.17)). Similarly, the expressions for the $c_i$ follow directly from the definition for the Alfven, slow and fast disturbance speeds (see equations (2.19)-(2.21)) on substituting for $\underset{\sim}{n}_j$ and $\underset{\sim}{H}$ the expressions

$$\underset{\sim}{n}_j = \cos\theta_j \underset{\sim}{N} + \sin\theta_j \underset{\sim}{x}_o, \tag{5.7}$$

$$\underset{\sim}{H} = H\cos\psi_H (\cos\theta_H \underset{\sim}{N} + \sin\theta_H \underset{\sim}{x}_o) + H\sin\psi_H \underset{\sim}{z}_o. \tag{5.8}$$

The corresponding formulas for the $U_{ij}$ and $c_{ij}$ may be obtained from equations (5.4)-(5.6) by the simple expedient of replacing r, b, $\psi_H$ and $\theta_H$ by r', b', $\psi_{H'}$ and $\theta_{H'}$ and replacing $\theta_i$ by the appropriate $\theta_{ij}$, j = 1,2, ... 6. In accordance with our previous notation, the indices j = 1,2 and 3 are to be associated with the reflected fast, Alfven and slow fronts respectively; and the indices j = 4, 5, and 6 with the slow, Alfven and fast transmitted waves.

Combining equation (4.1) and (4.2) with (4.3) and the corresponding formula for the scattered waves we find for each i, i = 1,2,3, that

$$(\underset{\sim}{V} - \underset{\sim}{u}_I) \cdot \underset{\sim}{n}_i = \pm c_i, \tag{5.9}$$

$$(\underset{\sim}{V} - \underset{\sim}{u}_I) \cdot \underset{\sim}{n}_{ij} = \pm c_{ij}, \qquad j = 1,2,3, \tag{5.10}$$

$$(\underset{\sim}{V} - \underset{\sim}{u}'_I) \cdot \underset{\sim}{n}_{ij} = \pm c_{ij}. \qquad j = 3,4,5. \tag{5.11}$$

Setting

$$\bar{V} = |\underset{\sim}{V} - \underset{\sim}{u}_I|, \tag{5.12}$$

and

$$\bar{V}' = |\underset{\sim}{V} - \underset{\sim}{u}'_I|, \tag{5.13}$$

and denoting by $\alpha$ and $\alpha'$ the angles that the velocities $\underset{\sim}{V} - \underset{\sim}{u}_I$ and $\underset{\sim}{V} - \underset{\sim}{u}'_I$ make with the surface normal at $\underset{\sim}{N}$, we arrive at the hydromagnetic analogue of Snell's laws; namely

$$\frac{|\cos(\theta_{ij} - \alpha)|}{c_{ij}} = \frac{|\cos(\theta_i - \alpha)|}{c_i} = \frac{1}{\bar{V}}, \quad j = 1,2,3, \tag{5.14}$$

$$\frac{|\cos(\theta_{ij} - \alpha)|}{c_{ij}} = \frac{|\cos(\theta_i - \alpha')|}{c_i} = \frac{1}{\bar{V}'}, \quad j = 4,5,6. \tag{5.15}$$

Introducing into these equations, the quantities

$$p_i = \frac{1}{c_i/b}\ , \tag{5.16}$$

$$p_{ij} = \begin{cases} c_{ij}/b, & j = 1,2,3 \\ c_{ij}/b', & j = 3,4,5. \end{cases} \tag{5.17}$$

and the Alfven numbers

$$M_b = \frac{1}{(\bar{V}/b)}\ , \tag{5.18}$$

$$M_b' = \frac{1}{\bar{V}'/b'}\ , \tag{5.19}$$

we may write Snell's laws in the following useful form:

$$p_{ij}\ |\cos(\theta_{ij} - \alpha)| = p_i\ |\cos(\theta_i - \alpha)| = \frac{1}{M_b}, \tag{5.20}$$

$$p_{ij}\ |\cos(\theta_{ij} - \alpha')| = p_i\ |\cos(\theta_i - \alpha')| = \frac{1}{M'_b}\ . \tag{5.21}$$

Regarding $(p_{ij}, \theta_{ij})$ as the polar coordinates of points in the $(p,\theta)$-plane, p being the radial variable, we see immediately that the $(p_{ij}, \theta_{ij})$, $j = 1,2,3$, all be on a line through $(p_i, \theta_i)$ whose equation is

$$\ell:\ \ p\ |\cos(\theta - \alpha)| = \frac{1}{M_b} = p_i\ |\cos(\theta_i - \alpha)| \tag{5.22}$$

while the $(p_{ij}, \theta_{ij})$, $j = 4,5,6$ all be on a line $\ell'$ through $(p_i, \theta_i)$ whose equation is

$$\ell':\ \ p\ |\cos(\theta - \alpha') = \frac{1}{M_{b'}} = p_i\ |\cos(\theta_i - \alpha')|\ . \tag{5.23}$$

Suppose now we plot $p_{ij}$, $j = 1,2,3$ against $\theta_{ij}$ on the same $(p,\theta)$ polar. The result is a family of five curves - the Alfven and slow curves consist of two branches each. It follows immediately from equations (5.20) and (5.22) that the points of intersection of the line $\ell$ with the curves of this family are solutions of equation (5.20) and hence furnish the angles of reflection and the reciprocal disturbance speeds of the reflected waves. These remarks are illustrated in Figure 9(a). The parameters $r$, $\theta_H$, $\psi_H$ and $\alpha$ are .5, $45^\circ, 0^\circ$ and $0^\circ$ respectively. Since $\alpha = 0$ the line $\ell$ is vertical. The distance of $\ell$ from the vertical $\underset{\sim}{N}$-axis is evidently $M_b^{-1}$. Figure 9(b) depicts the corresponding diagram for the transmitted waves.

We shall discuss our graphical method at greater length later. First, however, we wish to examine its relationship to Huygens' classical construction.

### B. Huygens' Construction of the Scattered Phase Fronts

We assume that the medium in $\mathcal{R}$ is at rest ($\underset{\sim}{u} = 0$) and consider the construction of the reflected fronts by Huygens' method which, in brief, is the following: At the instant the incident phase front reaches the point 0 of the interface (see Figure 7, 8), 0 becomes an induced point source and emits a wavelet or sphere (see Section II C). To construct the reflected phase fronts at time t' one simply constructs the envelopes of the spheres emitted at all times $t < t'$.

In Figure 10, 0' represents the trace point at time t' and 0 is the position $b^{-1}$ seconds earlier. It is assumed that 0' moves with the constant velocity $\underset{\sim}{V} = V \underset{\sim}{x}_o$ and that $V > 0$. The distance of 0' from O is therefore V/b. Taking r, $\psi_H$ and $\theta_H$ to be $\frac{1}{2}$, $0^\circ$ and $45^\circ$ respectively, the sphere through O is the surface of revolution obtained by revolving the $f_1$, $A_2$ and $s_3$-curves of the Figure 10 about the $\underset{\sim}{H}$-axis. The $\mathcal{W}_i$ in Figure 10 represents the three possible types of incident phase fronts and the $\mathcal{W}_{ij}$ represent the associated family of reflected phase fronts. The $\mathcal{W}_{ij}$ and the dashed extensions of the $\mathcal{W}_i$ are tangent to the $f_2$, $A_2$ and $s_3$-curves, since by construction these phase fronts must be the envelopes of the wavelets emitted earlier and up to $b^{-1}$ seconds later than the sphere shown. It is perhaps unnecessary to stress that the hemisphere in the transmission region $\mathcal{R}'$ indicates merely where the disturbance would have been were there no discontinuity across $\mathcal{D}$. The hemisphere through O appropriate to $\mathcal{R}'$, will in general, differ from that shown and as in geometrical optics may be employed in the construction of the transmitted phase fronts.

The geometry of Figure 10 changes only in an obvious manner when the parameters r, $\theta_H$ and V/b are varied. Thus the Alfven spheres are tangent to the $s_3$ or $f_1$ curves according as $r \geq 1$ or $r < 1$; but otherwise varying r effects only the detailed features of the figure. Varying $\theta_H$ has the effect of rotating the $f_1$, $A_2$ and $s_3$ curves rigidly about O. Finally, varying V/b moves O' closer to or farther from O and governs what may be termed the angles of "critical reflection" [15].

---

[15] A reflected front of type j due to a incident wave of type i is said to be critically reflected when $\theta_{ij}$ just becomes equal to ± $90^\circ$. The angle $\theta_i$ at which this occurs is called the angle of critical reflection for the j-wave.

For example, if O' falls with the $f_1$-oval, a fast phase front is not reflected since there are no tangents to the $f_1$-curve. In addition, we may mention an anomalous sort of reflection which occurs when O' coincides with O'' of Figure 10. In this case, it is easy to see that an incident slow front produces reflected slow and Alfven fronts which lie in the same quadrant as the incident wave itself. The flux of energy (see equation (3.14)) associated with each of these fronts is, however, in the proper direction, that is, away from the interface .

It has thus far been assumed that $\underset{\sim}{H}$ lies in the plane of incidence i.e., that $\psi_H = 0$. Increasing $\psi_H$ away from zero has the effect of turning the $\underset{\sim}{H}$-axis, the axis of revolution of the wavelets, out of the plane of the page. The points of tangency with the wavelets of the incident and scattered fronts also move out of the plane of the page and are no longer coplanar. Although Huygens' method seems now to require three dimensional figures, it is nevertheless still possible to perform the construction by the procedure described above. One need only work with the projection onto the plane of incidence of the locus of points on the wavelets at which the normal $\underset{\sim}{n}$ is parallel to the plane of incidence. The parametric equations of this locus may be obtained from the ray equations (3.7)-(3.9) by substituting the expressions for $\underset{\sim}{n}$ and $\underset{\sim}{H}$ given in equations (5.7) and (5.8). Figure 11 depicts this locus for various values of $\psi_H$; r, and $\theta_H$ are again assumed to be 1/2 and $45^\circ$. The Alfven locii are not shown.

To explain the essential elements of the relationship of Huygens' construction to the graphical procedure of Section A, it will suffice to show how to obtain Figure 9 a from Figure 10; in both figures $r = 1/2$, $\theta_H = 45^\circ$ and $\psi_H = 0$. We maintain that Figure 9a may be obtained from Figure 10 by 1) constructing the pedal curves to the curves of Figure 10, and then inverting these pedal curves[16] with respect to the unit circle centered at O.

To justify this statement we note that the pedals $\ell_i$ from O to the curves $f_1$, $A_2$, $s_3$ are $\ell_i = b^{-1} c_i(\underset{\sim}{n}_i)\underset{\sim}{n}_i$, $i = 1,2,3$, $\underset{\sim}{n}_i$ being the normal to the i-th curve. This fact follows from the way the wavelets are constructed and the fact that Figure 10 corresponds to an elapsed time $b^{-1}$ $(= t'-t)$ seconds. The inverse point of $\ell_i$ with respect to the unit circle at O is evidently the vector directed along $\underset{\sim}{n}$ of length

$$p_i = \frac{1}{c_i(\underset{\sim}{n}_i)/b}, \quad i = 1,2,3 \tag{5.24}$$

Comparing this equation with equation (5.16), we conclude with aid of equations (5.7) and (5.8) that the corresponding $(p,\theta)$-polars and are in fact those shown in Figure 9(a).

---

[16] The pedal curve of a curve C, whose equation is $\underset{\sim}{x} = \underset{\sim}{x}(\xi)$, is constructed as follows: Let $T(\xi)$ be the tangent to C. From the origin O, draw the perpendicular to $T(\xi)$ and let $\underset{\sim}{y} = \underset{\sim}{y}(\xi)$ denote the vector from O to the foot of this perpendicular. The curve traced out by $\underset{\sim}{y}$ as $\xi$ varies over its domain of definition is the pedal curve of $\zeta$.

To complete the picture we consider the family of lines through O'. This family of lines includes, among others, the lines representing the six wave fronts. Let $\theta$ be the angle that the normal to a line of the family makes with the vertical N-axis through O'. In Figure 10, for example, $\theta_3$ is the angle that the slow wave front makes with the N-axis. Then, it is easy to verify that (1) the pedal curve of each line of the family consists of a single point with the polar coordinates $(q,\theta) = (\frac{V}{b}\sin\theta, \theta)$ and (2) the locus of these points is a circle of diameter V/b whose equation is

$$q = \frac{V}{b}\sin\theta. \tag{5.25}$$

If we invert this circle in the unit circle - i.e., if we replace q by 1/p, we find that

$$p \sin\theta = \frac{1}{V/b}\ , \tag{5.26}$$

which is precisely the equation of the line $\ell$ of equation (5.22) when, as is the case, here $\alpha = 0$.

## C. The Graphical Method

Although Huygens' construction has greater physical appeal, the graphical method outlined at the end of subsection A has much in its favor. First, it is more accurate; for a point of intersection is more easily located than a point of tangency. Second, as the angles of reflection and refraction and corresponding (reciprocal) disturbance speeds are determined simultaneously, it yields more information. Finally, the avoidance of the cusped figures should be noted.

In Figures 12(a)-(c) we show polar plots for $r = 1/2$ (Figure 12(a), $r = 1$ (Figure 12(b)) and $r = 2$ (Figure 12(c)). In all cases, $\alpha = 0$ $\theta_H = 45^\circ$ and $\psi_H = 0$. Figure 12(c) also contains curves associated with the parameter values $r = 2$, $\theta_H = 45^\circ$ and $\psi_H = 45^\circ$; we shall have occasion to refer to these later. As in Figure 8, all angles are measured from the vertical $\underset{\sim}{N}$-axis and are considered positive or negative according as they are measured clockwise or counterclockwise from $\underset{\sim}{N}$.

Whatever the value of r, the oval-like curves (labelled $f_1$) correspond to the fast $p_{i1}$- branch; the pair of solid lines (labelled $A_2$), perpendicular to the $\underset{\sim}{H}_I$-axis, correspond to the Alfven $p_{i2}$- branch and the hyperbola-like curves (labelled $s_3$) correspond to the $p_{i3}$-slow branch. The pair of interrupted lines, perpendicular to the $\underset{\sim}{H}_I$-axis are the loci of points satisfying the equation.

$$p b \cos \psi_H \left|\cos (\theta - \theta_H)\right| = \left[(1 + r)/r\right]^{\frac{1}{2}} \qquad (5.27)$$

These lines serve as asymptotes of the $s_3$-curves. The $f_1$, $A_2$ and $s_3$-curves are all symmetric with respect to the origin and with respect to the $\underset{\sim}{H}_I$-axis. It follows directly from equation (5.17) and the corresponding equations for the $c_{ij}/b$ that when $\psi_H = 0$ the Alfven branch intersects the slow branch, the fast branch or both according as r exceeds unity, is less than unity or equal to unity. All branches have zero curvature on the $H_I$-axis when $r \neq 1$. When $r = 1$, both the slow and fast branches are singular on the $\underset{\sim}{H}_I$-axis. They have points in common at $p = 1$, $\theta = \theta_H$ and $p = 1$, $\theta = \theta_H + \pi$ and at each of these points are tangent to a pair of lines that make an angle of $\Phi = \pm \tan^{-1}(1/2)$ with the $\underset{\sim}{H}$-axis. [See Figure 12(b)]. By rotating the curves of Figures 12(a), (b), or (c) about the $\underset{\sim}{H}_I$ = H-axis we arrive at a family of surfaces in p-space known collectively as the surface of phase normals.

The curves of Figures 12(a)-(c) are typical of those in the parameter classes $r > 1$, $r = 1$ and $r < 1$, respectively. Keeping r and $\theta_H$ fixed, and increasing $\psi_H$, we find from the equations for the $c_{ij}/b$ (cf. equation (4.4)-(4.7)) that for each $\theta$, that the points on the $f_1$-curves move toward the origin and the points on the $A_2$ and $s_3$-curves move away from the origin. The general appearance of these curves, however, remains the same as in the case $\psi_H = 0$ [see, e.g., the curves of Figure 11(c) associated with $\psi_H = 45^\circ$] except on and in the neighborhood of the $H_I$-axis. Here, the double or triple points - i.e., the points where the Alfven wave intersects the slow branch $(r > 1)$, the fast branch $(r = 1)$ or both $(r = 1)$ - split up into two and three separate points respectively. Moreover, in the case $r = 1$, the curvatures of the slow and fast branches on the $H_I$ axis are no longer singular. Finally, we note that the sole effect of varying $\theta_H$ while keeping r and $\psi_H$ fixed is to rotate the $f_1$, $A_2$ and $s_3$-curves rigidly with respect to the fixed axes along $\underset{\sim}{N}$ and $\underset{\sim}{x}_0$.[17]

---

[17] Rather than draw a new set of s, A and f-curves for each new $\theta_H$, it is evidently simpler in numerical work to deal with one fixed set of curves and to rotate the $\underset{\sim}{N}$-axis with respect to this fixed set in such a manner that $\underset{\sim}{H}_I$ makes an angle $\theta_H$ with $\underset{\sim}{N}$.

The effect of varying the angular parameters $\psi_H$ and $\theta_H$ may be visualized as changing the orientation of the surface of wave normals with respect to the plane of incidence.

Let us again focus on the problem of reflection and assume once more that $\alpha$ vanishes. It may be imagined here that the undisturbed medium in $\mathcal{R}$ is motionless and that $\mathcal{D}$ is a rigid surface. In this case, as we pointed out earlier, the line $\ell$ is parallel to the $\underset{\sim}{N}$-axis; its distance from the $\underset{\sim}{N}$-axis is evidently the reciprocal of the Alfven number.

By varying the angle of incidence and counting the number of intersections of $\ell$ with the lower portions of the $f_1$, $A_2$, $s_3$-curves, one arrives at the following conclusions: (see Figure 9a), (1) For sufficiently small angles of incidence (and correspondingly large Alfven numbers) there are three (real) angles of reflection[18] $\theta_{i1}$, $\theta_{i2}$ and $\theta_{i3}$. (2) To each fast incident wave with sufficiently small $|\theta_1|$ there corresponds three such angles of reflection. However, when $\theta_1$ is approximately 70° the fast reflected wave is critically reflected.[19] (3) When the incident wave is of the slow or Alfven type then at positive and negative angles of incidence which are sufficiently large in absolute value, the fast wave is critically reflected. (4) At sufficiently large positive angles of incidence, Alfven or slow waves can produce at most two real reflected waves - one Alfven and one slow wave. The same is true of negative angles of incidence which are moderate in absolute value. (5) However, at negative angles of incidence that become successively larger in absolute value, first the Alfven and then the slow wave is critically reflected.

---

[18] Whether or not the associated modes of propagation are excited or not depends upon the boundary conditions and on the orientation of the magnetic field.

[19] See footnote 15.

Statements (1)-(5) refer specifically to Figure 9(a). However, with obvious changes they apply for all values at r, $\psi_H$ and $\theta_H$, the angles $\psi_H = \pm 90^\circ$, $\pm 180^\circ$ excepted. Statement (5) is no longer valid in the exceptional cases; but (1)-(4) still apply with minor changes. The reader is referred to reference [23] Figure 4(b) for numerical results and in addition for a detailed analysis of the problem of refraction.

### D. General Properties of the Angles of Reflection

The angles of reflection in the problem discussed above enjoy several general properties which are consequences of the particular way in which the ratios $c_{ij}/b$, i,j = 1,2,3, depend upon $\theta_i$, r, $\theta_H$ and $\psi_H$. We wish to present some of these now.

Let

$$\theta_{ij} = \Theta_{ij}\left[\theta_i;\ \theta_H,\ \psi_H,\ r\right] \qquad i,j = 1,2,3, \tag{5.28}$$

express the functional relationship between $\theta_{ij}$, $\theta_i$ and $\theta_H$, $\psi_H$ and r. Then the following properties can be shown to follow from Snell's laws which, in the present case, are

$$\frac{\sin\theta_{ij}}{c_{ij}/b} = \frac{\sin\theta_i}{c_i/b} \qquad i,j = 1,2,3, \tag{5.29}$$

and the expressions for the distrubance speeds (see equations (5.3)-(5.5)).

$$
\begin{array}{llr}
\textcircled{H}_{ij}\,[\psi_H] = \textcircled{H}_{ij}\,[-\psi_H], & & A_1 \\
\textcircled{H}_{ij}\,[\theta_H \pm \pi] = \textcircled{H}_{ij}\,[\theta_H]\;, & & A_2 \\
\textcircled{H}_{ij}\,[r^{-1}] = \textcircled{H}_{ij}\,[r] & i,j = 1,3 & A_3 \\
\textcircled{H}_{ij}\,[-\theta_i;\, -\theta_H] = -\theta_{ij}, & & A_4 \\
\textcircled{H}_{ij}\,[-\theta_i;\, \theta_H] = -\,\textcircled{H}_{ij}\,[\theta_i;\, -\theta_H]\;, & & A_5 \\
\textcircled{H}_{ij}\,[-\bar{\theta}_{ij}] = -\begin{cases} \pi - \theta_i, \text{ if } \theta_i > 0 \\ -(\pi + \theta_i), \text{ if } \theta_i < 0; \end{cases} & j = 1,2,3, & A_6 \\
|\bar{\theta}_{i1}| \geq |\bar{\theta}_{i2}| \geq |\bar{\theta}_{i3}|, & & A_7
\end{array}
\qquad (5.30)
$$

In these relations, parameters not shown are considered fixed and unless specifically indicated otherwise the subscripts i and j assume the values 1,2,3. The angles $\bar{\theta}_{ij}$ appearing in equations $A_6$ and $A_7$ are what we shall hereafter refer to as the acute angles of reflection. They are defined as follows:

$$
\bar{\theta}_{ij} = \begin{cases} \pi - \theta_{ij}, \text{ if } \theta_{ij} > 0 \\ -(\theta_{ij} + \pi), \text{ if } \theta_{ij} < 0 \end{cases} , \quad \begin{array}{l} i = 1,2,3, \\ j = 1,2,3, \end{array} \qquad (5.31)
$$

Equation $A_1$ expresses the fact that the angles of reflection are independent of the direction of the component of $\underset{\sim}{H}$ which is perpendicular to the plane of incidence. Equation $A_2$ states that these angles are also independent of the sense of $\underset{\sim}{H}_I$. Together, $A_1$ and $A_2$ imply that the reflected angles are independent of the sense of $\underset{\sim}{H}$. Equation $A_3$ states that the slow and fast angles of reflection are invariant under the transformation of $r \rightarrow r^{-1}$ whenever the incident wave is slow or fast. From $A_4$ we conclude that if a wave incident at the angle $\theta_i$ produces scattered waves at the angles $\theta_{ij}$, then a wave incident at the angle $-\theta_i$ will produce scattered waves at the angles $-\theta_{ij}$ only if the direction of $\underset{\sim}{H}_I$ is reflected in the $\underset{\sim}{N}$-axis; specifically, only if $\theta_H$ is replaced by $-\theta_H$. If $\theta_H$ is not so replaced, then according to $A_5$ the scattered waves emerge at the new angles $\theta^*_{ij} = -\textcircled{H}_{ij}\left[-\theta_i;\ \theta_H\right]$, which differ, in general, from $-\theta_{ij}$. Only when $\theta_H$ is $0^\circ$, $\pm 90^\circ$ and $180^\circ$ do we find that $\theta^*_{ij} = -\theta_{ij}$. In other words, negative angles of incidence are not physically equivalent to positive angles of incidence except for special orientations of the magnetic field.

Equation $A_6$ expresses the reversibility of the reflection process in the following sense. If $\overline{\theta}_{ij}$ is the acute angle of reflection of a front of type j due to an incident front of type i, then a front of type j incident of the angle $-\overline{\theta}_{ij}$ will produce a reflected front of type i which emerges at the angle of incidence $\theta_i$ propagating in the direction opposite to that of the original incident front. In $A_8$, it is assumed that the $\overline{\theta}_{ij}$ are real. These relations affirm a fact to be expected on physical grounds; namely, that the fast reflected fronts emerge first, followed by the Alfven front, and then the slow front.

The analogues of $A_1$-$A_8$ for the angles of refraction in the case which $\alpha'$ vanishes in the transmission region will be found in reference [23].

## E. Explicit Formulas for Alfven Waves at a Contact Discontinuity

Suppose the surface of discontinuity $\mathcal{D}$ is a hydromagnetic contact discontinuity. As is well known,[13] only the density and entropy may be discontinuous across a hydromagnetic contact discontinuity, unless $H_N$, the normal component of the magnetic field vanishes. When $H_N$ vanishes, a discontinuity of $\underset{\sim}{u}$ across $\mathcal{D}$ is permissible; however, it will be assumed below that $\underset{\sim}{u}$ is continuous across $\mathcal{D}$ in this exceptional case too. From the Galilean invariance of the jump relations, it follows that $\underset{\sim}{u}$ may, without loss of generality be assumed to vanish everywhere. We assume below that this is the case.

Suppose now that an Alfven front is incident at the angle $\theta_2$. We wish to derive the acute angle of reflection $\bar{\theta}_{22}$ (see equation (5.31)) and the angle of refraction $\theta_{22}$ at which the scattered *Alfven* fronts emerge.[20] The solution of this problem follows almost immediately from Snell's laws (equation (4.29)) and equation (5.5) which implies the formulas ($\theta_H \neq \pm 90^\circ$)

$$\operatorname{ctn} \bar{\theta}_{22} = \operatorname{ctn} \theta_2 + 2 \tan \theta_H, \qquad (5.32$$

---

[20] When $\underset{\sim}{H}$ is not in the plane of incidence, slow and fast fronts will be scattered from $\mathcal{D}$. Explicit formulas for the angles corresponding to these waves are however difficult to obtain.

$$\operatorname{ctn}\theta_{24} = \eta^{\frac{1}{2}}\operatorname{ctn}\theta_2 + (\eta^{\frac{1}{2}} - 1)\tan\theta_H, \tag{5.33}$$

where

$$\eta = b/b' = (\rho'/\rho)^{\frac{1}{2}} \tag{5.34}$$

It should be stressed that these formulas are valid for all values of $\psi_H$ between ± 90°; i.e., $\underset{\sim}{H}$ need not lie in the plane of incidence. It is therefore noteworthy that $\theta_{22}$ and $\theta_{24}$ depend only on $\theta_H$, the angle that $\underset{\sim}{H}_I$, the projection of $\underset{\sim}{H}$ on the plane of incidence, makes with the normal. This interesting fact seems to have been overlooked by V.C.A. Ferraro[1] who derived another somewhat more complicated pair of equations.

To relate Ferraro's equations to ours, we refer to Figure 7 and note the following relations between $\theta_H$ and the polar angles $\beta$ and $\gamma$ employed by him:

$$H_I \cos\theta_H = H \sin\beta$$

$$H_I \sin\theta_H = H \cos\beta \cos\gamma.$$

These, in turn, imply the relation

$$\tan\theta_H = \operatorname{ctn}\beta \cos\gamma$$

which, combined with equations (5.32) and (5.33) yields Ferraro's results - apart from obvious notational differences.

In Figure 13 we have plotted $\bar{\theta}_{22}$ against $\theta_2$ for $\theta_H = 0^\circ$, $\theta_H = 45^\circ$ and $\theta_H = -45^\circ$. These are typical curves in the parameter classes $\theta_H = 0$, $\theta_H > 0$ and $\theta_H < 0$, respectively.

The angle

$$\bar{\theta}^*_{22} = \operatorname{ctn}^{-1}\left[\, 2\tan\theta_H \right] \tag{5.35}$$

introduced in Figure 13 is the maximum positive angle of reflection when $\theta_H$ is positive and the minimum negative angle of reflection when $\theta_H$ is negative. For a given $\theta_H$,

$$\theta_2^\dagger = \mathrm{ctn}^{-1} \left[ -2 \tan \theta_H \right] \tag{5.36}$$

gives the critical angle of reflection; it is evidently positive when $\theta_H$ is negative and negative when $\theta_H$ is positive. Not shown in Figure 12 are the angles of reflection associated with angles of incidence $\theta_2$ which produce anomalous reflection as defined in the previous section. These, to be sure, may also be computed from equation (5.32) and (5.33). Consider, for example, the curves of Figure 13. Here, one can obtain the anomalous values of $\bar{\theta}_{22}$ by including values of $\theta_2$ in the range $\theta_2^\dagger < \theta_2 \leq 45^\circ$ when $\theta_H = -45^\circ$ and by including values of $\theta_2$ in the range $\theta_2^\dagger > \theta_2 \geq -45^\circ$ when $\theta_H = 45^\circ$. In the first case $\bar{\theta}_{22}$ will take on anomalous values between $90^\circ$ and $135^\circ$ while in the second case $\bar{\theta}_{22}$ will take on anomolous values between $-90^\circ$ and $-135^\circ$. In both cases the reflected fronts will be found in the same quadrant as the incident front. The reader is referred to reference [22] for a discussion of equation (5.33) and associated graphs, and to references [7], [22], [23] for a derivation of the coefficients of reflection and refraction.

# APPENDIX I

## Variation of the Strengths of the Fundamental Waves Along Their Rays

The first two equations in the recursive matricial system (2.12)-(2.13) are

$$(M - \rho^{\frac{1}{2}} c\ I)\ \delta R^{(0)} = 0\ , \tag{I.1}$$

$$(M - \rho^{\frac{1}{2}} c\ I)\ \delta R^{(1)} = (\delta R^{(0)})\ , \tag{I.2}$$

where $\delta R^{(k)}$ is defined in equation (2.15). Now let $\delta R^{(0)}$ be any one of the six solutions $\epsilon_s^{\pm} R_s^{\pm}$, $\epsilon_A^{\pm} R_A^{\pm}$, $\epsilon_f^{\pm} R_f^{\pm}$ of (I.1) introduced in Section II (see equation (2.28)) and let c denote the corresponding disturbance speed. Since M is symmetric and since the left member of (I.2) has the same matrix as the left member of (I.1), it follows that (I.2) has a solution if and only if the six vector $P(\delta R^{(0)})$ is perpendicular to $\delta R^{(0)}$. This condition, written out explicitly with the aid of equation (2.15) reduces after some manipulation to the orthogonality condition of reference [1a,b]; namely,

$$\begin{aligned} 0 = \nabla \cdot \underset{\sim}{F} + \rho\ \delta \underset{\sim}{u}^{(0)} \cdot (\delta \underset{\sim}{u}^{(0)} \cdot \nabla)\underset{\sim}{u} - \tfrac{1}{2} \frac{(\delta \rho^{(0)})^2}{\rho} (\underset{\sim}{u} \cdot \nabla)\ a^2 \\ + \tfrac{1}{2} \mu\ (\delta H^{(0)})^2\ \nabla \cdot \underset{\sim}{u} - \mu\ \delta H^{(0)} \cdot (\delta \underset{\sim}{H}^{(0)} \cdot \nabla)\ \underset{\sim}{u}\ . \end{aligned} \tag{I.3}$$

In this equation, $\underset{\sim}{F}$ is the flux vector (see equation (2.5')) associated with the given fundamental wave.

Note that $\delta \underset{\sim}{H}^{(0)}$, $\delta \underset{\sim}{u}^{(0)}$ and $\delta \rho^{(0)}$ are linear in the strength $\epsilon$ (cf. equations (2.24) - (2.25)) of the wave. We may therefore cast equation (I.3) into the form

$$\nabla \cdot \underset{\sim}{F} + \epsilon^2 \underset{\sim}{I} = 0 \ , \tag{I.4}$$

where $\underset{\sim}{I}$ is a vector which is independent of $\epsilon$. Now we have seen (equation (3.14)) that the relation

$$\underset{\sim}{F} = \epsilon^2 \underset{\sim}{v} \ , \tag{I.5}$$

$\underset{\sim}{v}$ denoting the ray velocity, obtains in each of the six fundamental waves. Combining this relation and equation (I.4), we find that

$$\underset{\sim}{v} \cdot \nabla \epsilon^2 + \epsilon^2 \left[ \nabla \cdot \underset{\sim}{v} + I \right] = 0. \tag{I.6}$$

But, it follows from simple geometric considerations (see equation (4.6) that

$$\nabla \cdot \underset{\sim}{v} = \frac{d}{dt} \left[ \log \left( AU/U_o \right) \Big|_{\underset{\sim}{x} = \underset{\sim}{x}(t)} \right] . \tag{I.7}$$

Here, A is the expansion ratio defined in equation (3.21), U is the normal velocity of the phase front at time t, $U_o$ is the normal velocity at time $t = t_o$ and $\underset{\sim}{x} = \underset{\sim}{x}(t)$ is the equation of the ray. Substituting this expression for $\nabla \cdot \underset{\sim}{v}$ into equation (I.5) and noting that $\underset{\sim}{v} \cdot \nabla \epsilon^2$ is the derivative of $\epsilon^2$ along $\underset{\sim}{x} = \underset{\sim}{x}(t)$ (i.e., that $\underset{\sim}{v} \cdot \nabla \epsilon^2 = d\epsilon^2/dt$) we obtain $\epsilon^2$ along $\underset{\sim}{x} = \underset{\sim}{x}(t)$ as a solution of the first order linear differential equation

$$\frac{d\,\epsilon^2}{d\,t} + \epsilon^2 \left\{ I + \frac{d}{dt} \left[ \log \left( AU/U_o \right) \right]_{\underset{\sim}{x} = \underset{\sim}{x}(t)} \right\} = 0. \tag{I.8}$$

The expressions for $\epsilon^2$ catalogued in Section III B in equations (3.17)-(3.20) were obtained in this fashion.

We observe finally that the only complex quantity in equation (I.8) is $\epsilon^2$ (= $|\epsilon^2| \exp(2i\,\phi)$ say). It follows immediately that $\frac{d\,\phi}{d\,t}$ vanishes along the ray.

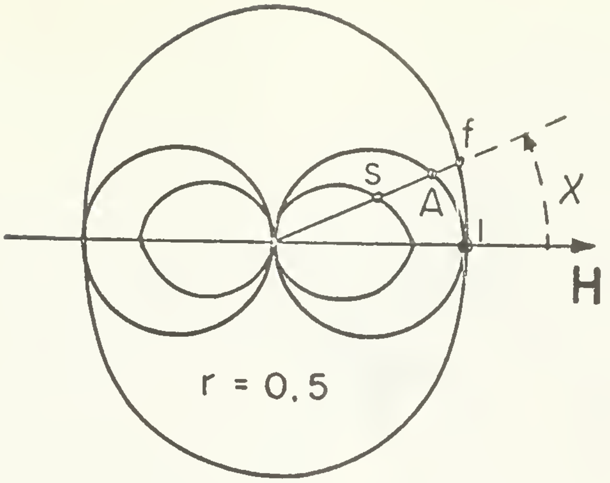

Figure 1. Cross-sectional view of the surface of normal speeds for the parameter value $r = 1/2$.

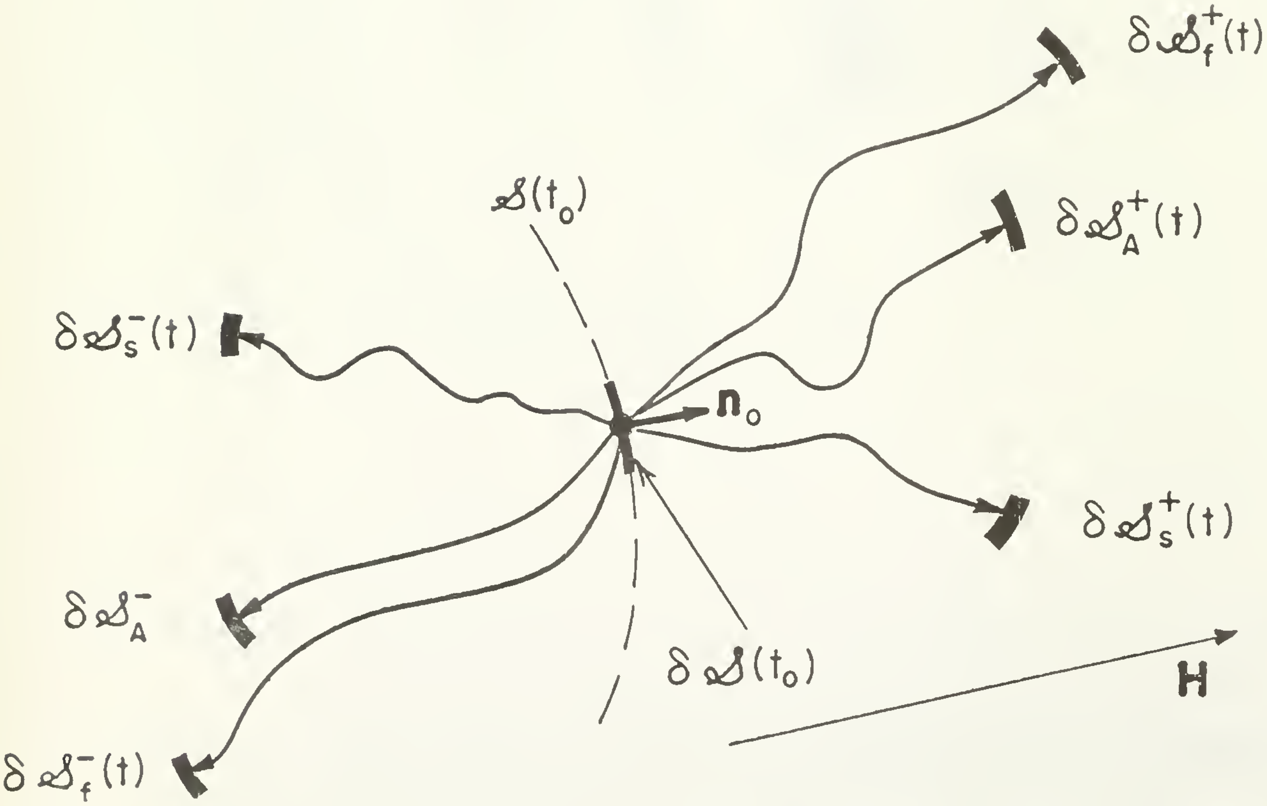
$\delta\mathscr{S}_f^+(t)$
$\delta\mathscr{S}_A^+(t)$
$\mathscr{S}(t_o)$
$\delta\mathscr{S}_s^-(t)$
$\mathbf{n}_o$
$\delta\mathscr{S}_s^+(t)$
$\delta\mathscr{S}_A^-$
$\delta\mathscr{S}(t_o)$
H
$\delta\mathscr{S}_f^-(t)$

Figure 2. Illustration of the splitting up of phase front element $\delta\mathscr{S}(t_o)$ into the three forward propagating elements $\delta\mathscr{S}_i^+(t)$, $i = s, A, f$ and three backward propagating elements $\delta\mathscr{S}_i^-(t)$, $i = s, A, f$.

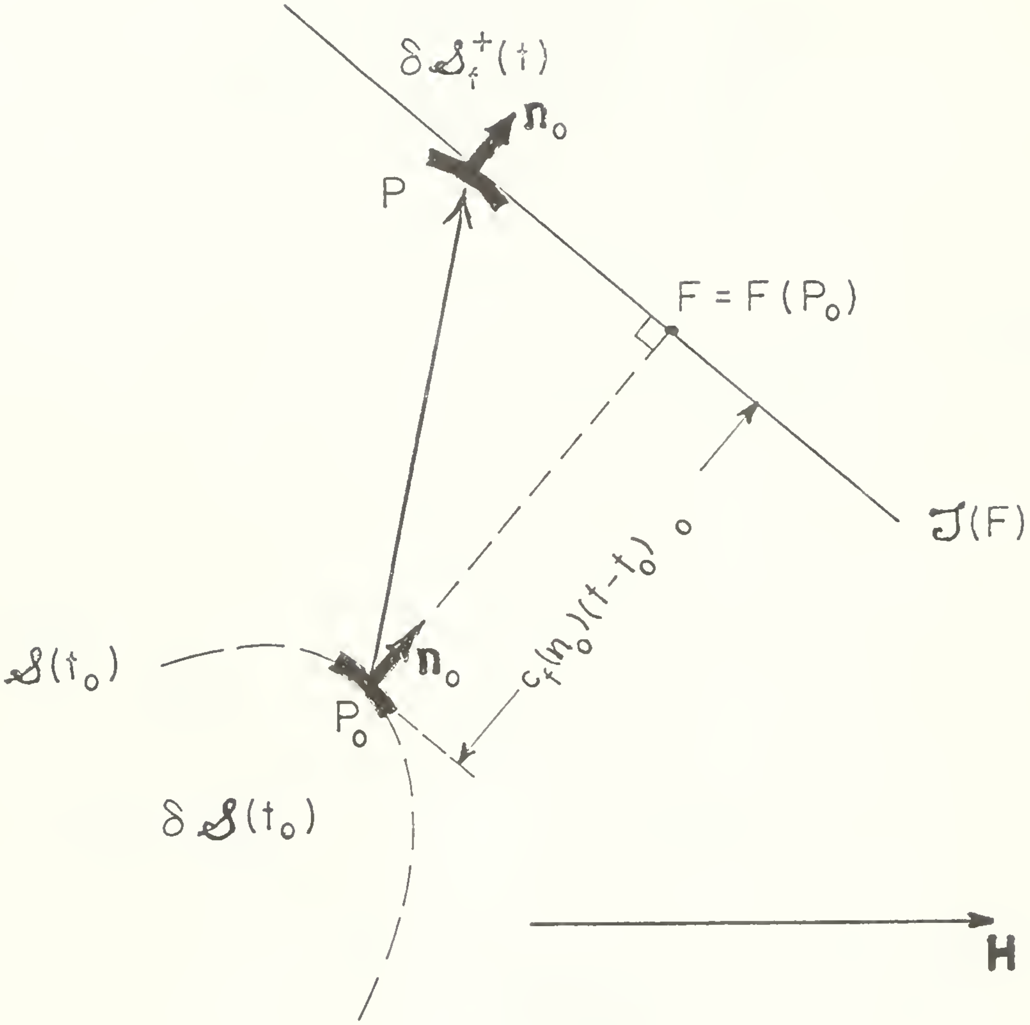

Figure 3. Construction of the fast phase front $\mathscr{S}^+_f(t)$ evolving out of the initial front $\mathscr{S}(t_o)$ in the case where the unperturbed flow is spacially uniform. The envelope of the planes T(F) determines the phase front at time t.

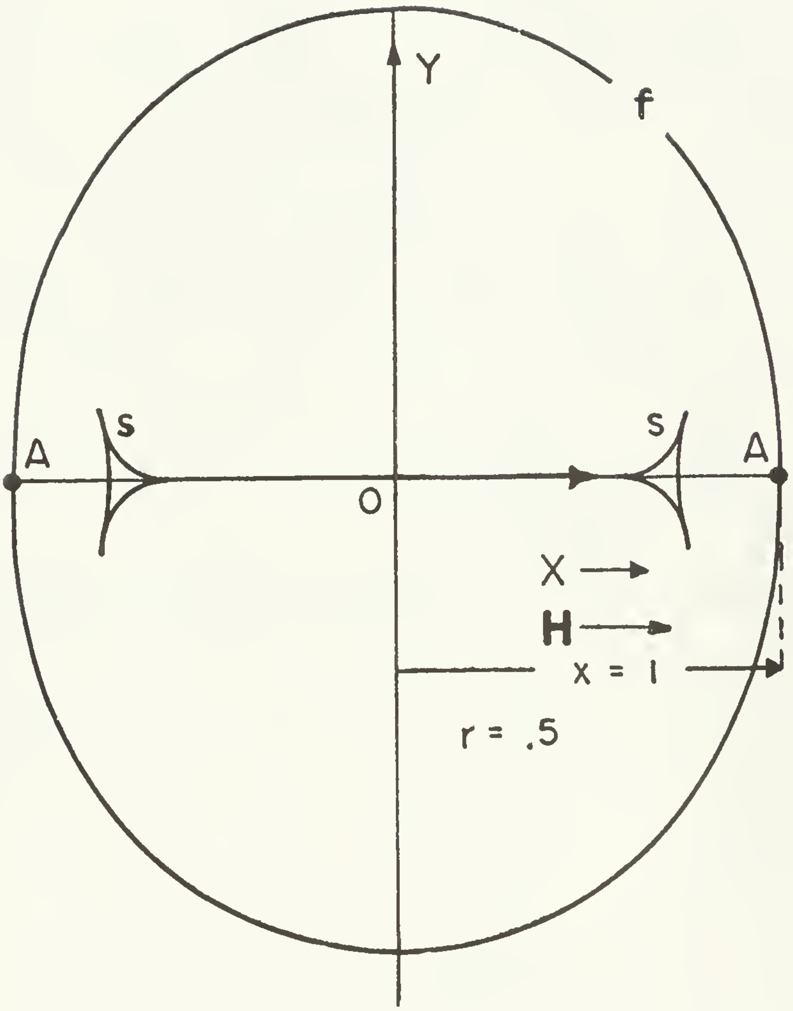

Figure 4. The Friedrichs' ray surface. This figure depicts the phase fronts that emerged from a point source at O, $b^{-1}$ seconds earlier. The ray surface is obtained by revolving the figure about the $\underset{\sim}{H}$-axis. It is the analogue of Fresnel's ray surface in optics. The undisturbed medium is assumed to be uniform.

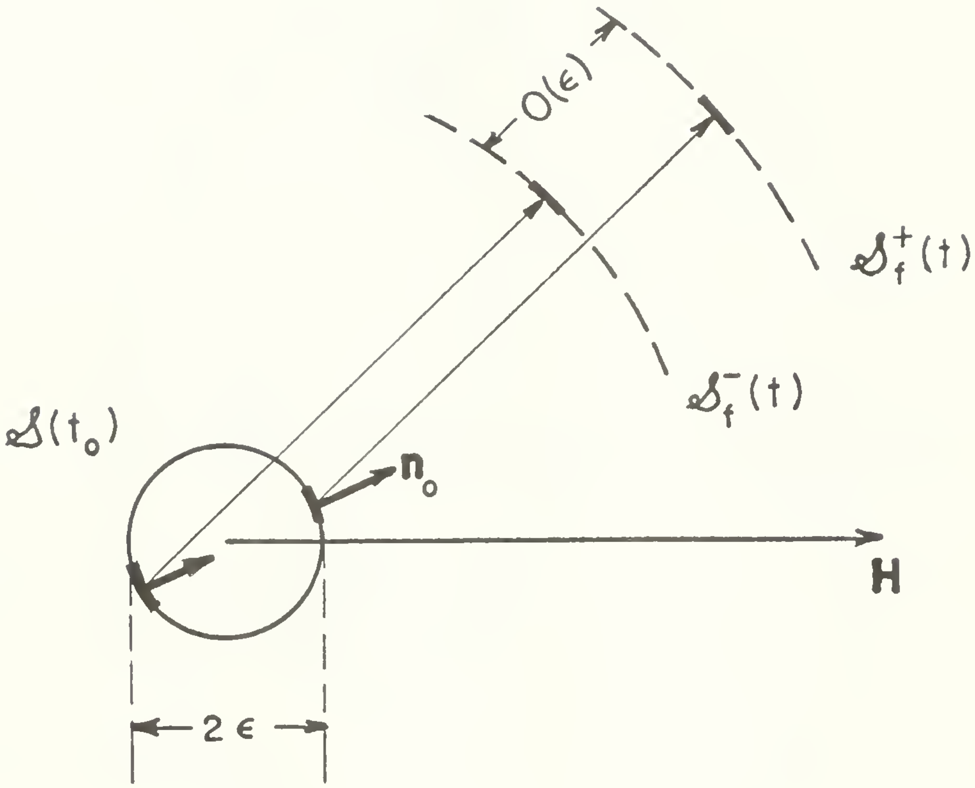

Figure 5. Illustration of the fact that $\mathcal{S}_f^-$ and $\mathcal{S}_f^+$ emerging from a spherical source of (small) diameter $2\epsilon$ are actually distinct phase fronts or order $2\epsilon$ apart.

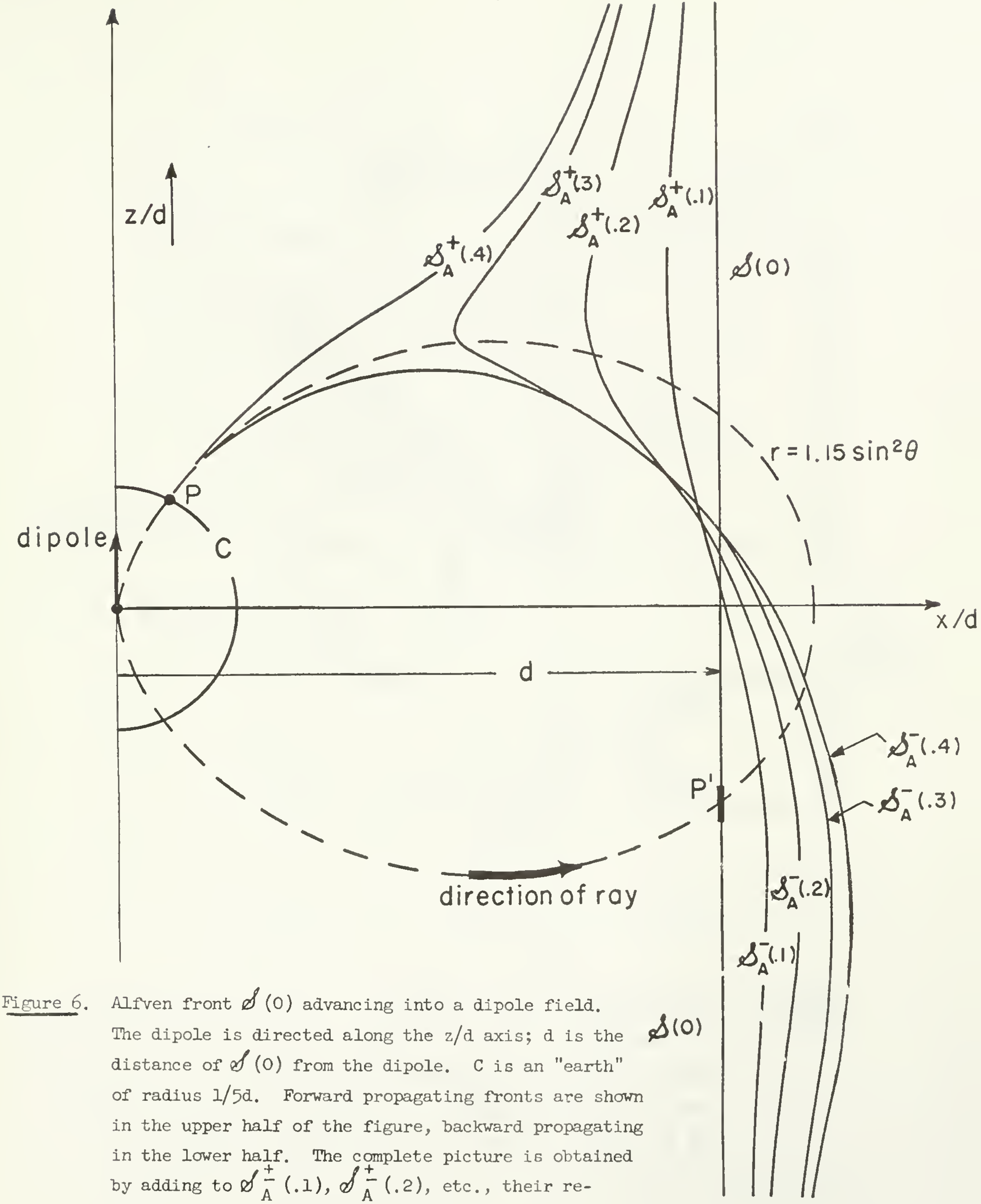

Figure 6. Alfven front $\mathcal{S}(0)$ advancing into a dipole field. The dipole is directed along the z/d axis; d is the distance of $\mathcal{S}(0)$ from the dipole. C is an "earth" of radius 1/5d. Forward propagating fronts are shown in the upper half of the figure, backward propagating in the lower half. The complete picture is obtained by adding to $\mathcal{S}_A^{\pm}(.1)$, $\mathcal{S}_A^{\pm}(.2)$, etc., their reflections in the x/d axis. A distinct peak forms at "time" $\tau = .4$.

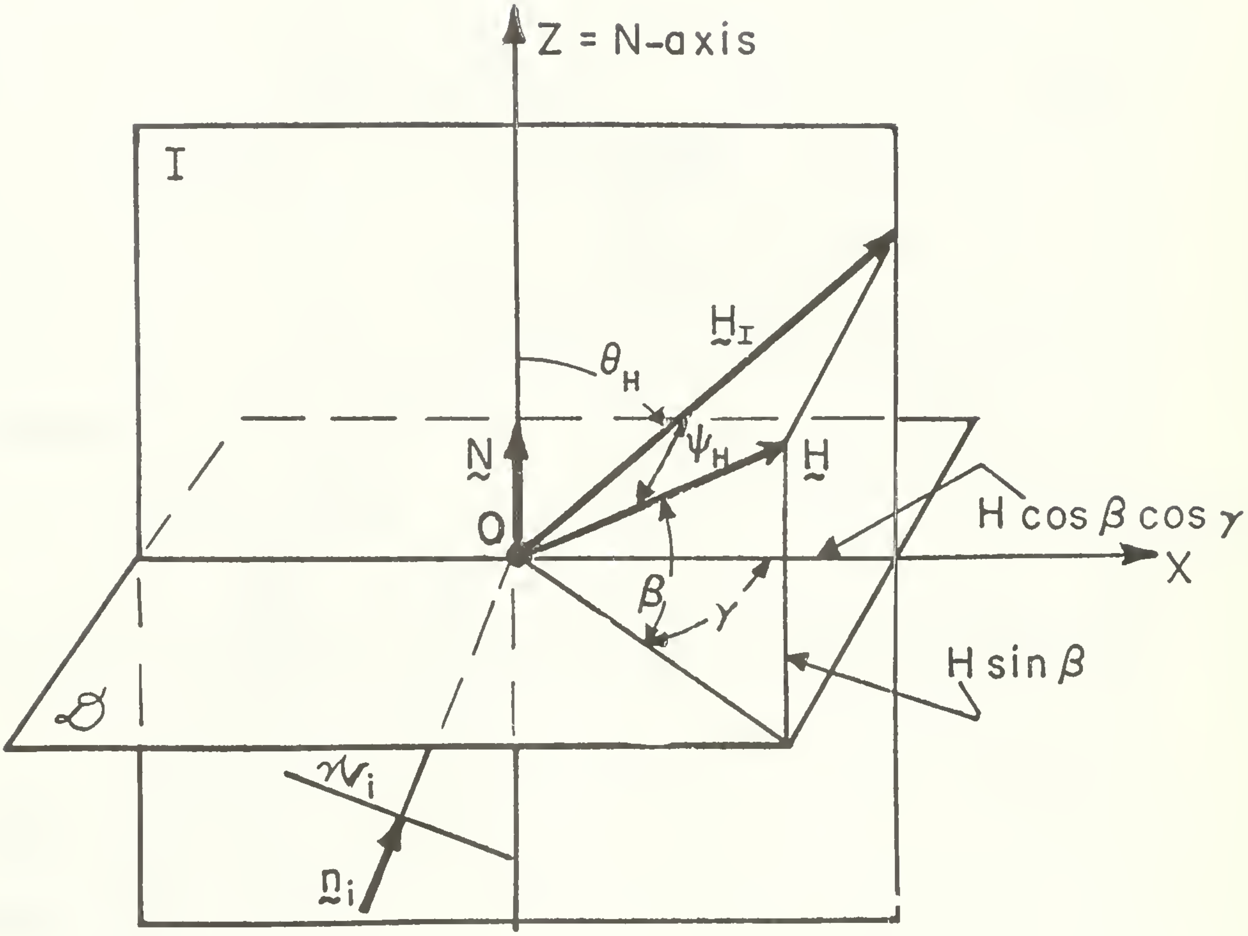

Figure 7. An incident wave $\mathcal{W}_i$ impinging on a surface of discontinuity $\mathcal{D}$. The plane I, defined by the normal $\underset{\sim}{n}_i$ to the incident wave and the normal $\underset{\sim}{N}$ is the plane of incidence. $\underset{\sim}{H}_I$ is the projection of $\underset{\sim}{H}$ on the plane of incidence. The angle between $\underset{\sim}{H}$ and $\underset{\sim}{H}_I$ is $\psi_H$. The angle (in I) between $\underset{\sim}{H}_I$ and $\underset{\sim}{N}$ is $\theta_H$.

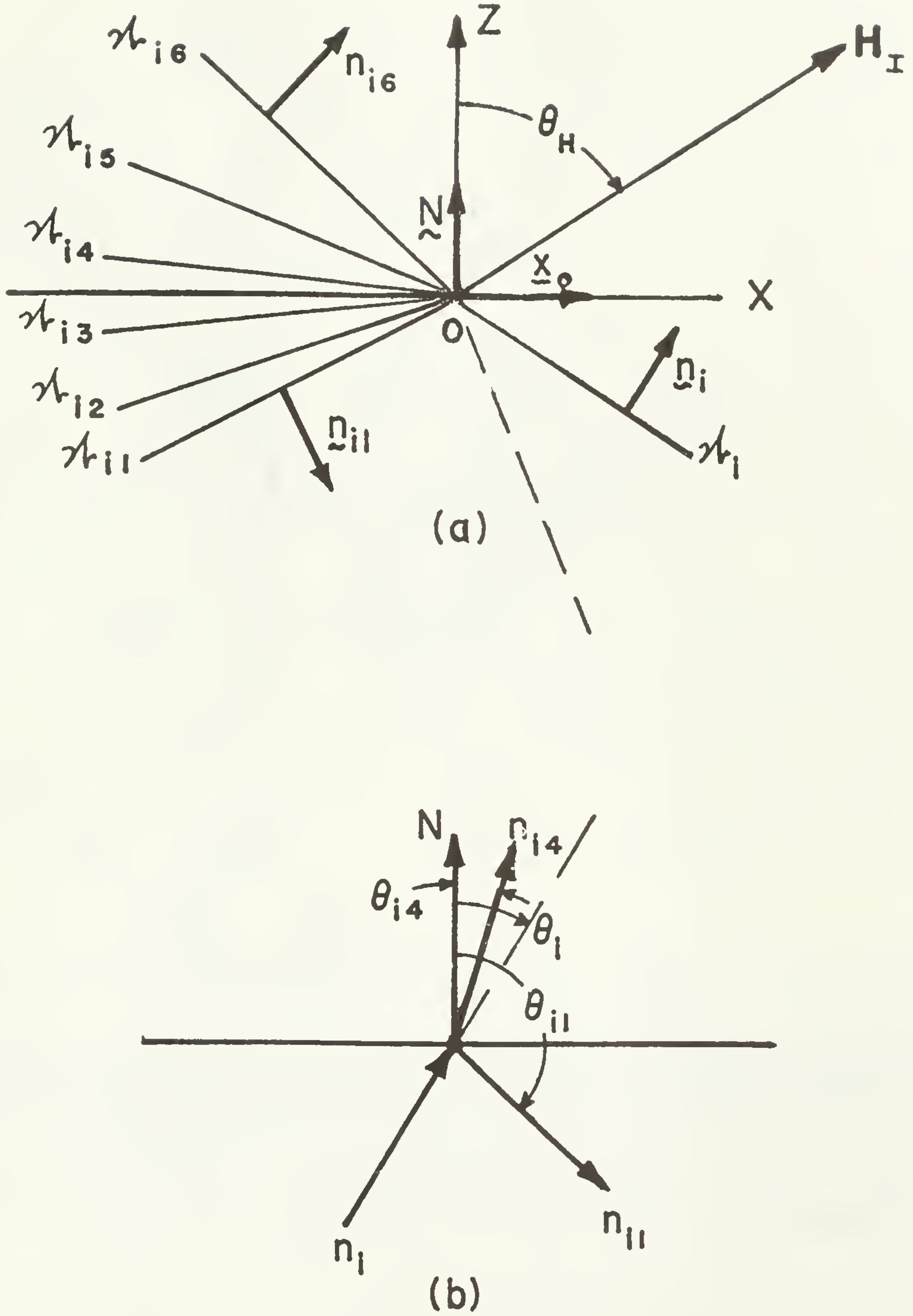

Figure 8 (a). The disposition of the phase fronts in the plane of incidence.

(b) The orientations of the normals to the phase fronts $\mathcal{W}_i$, $\mathcal{W}_{i4}$ and $\mathcal{W}_{i1}$ of Figure 8(a).

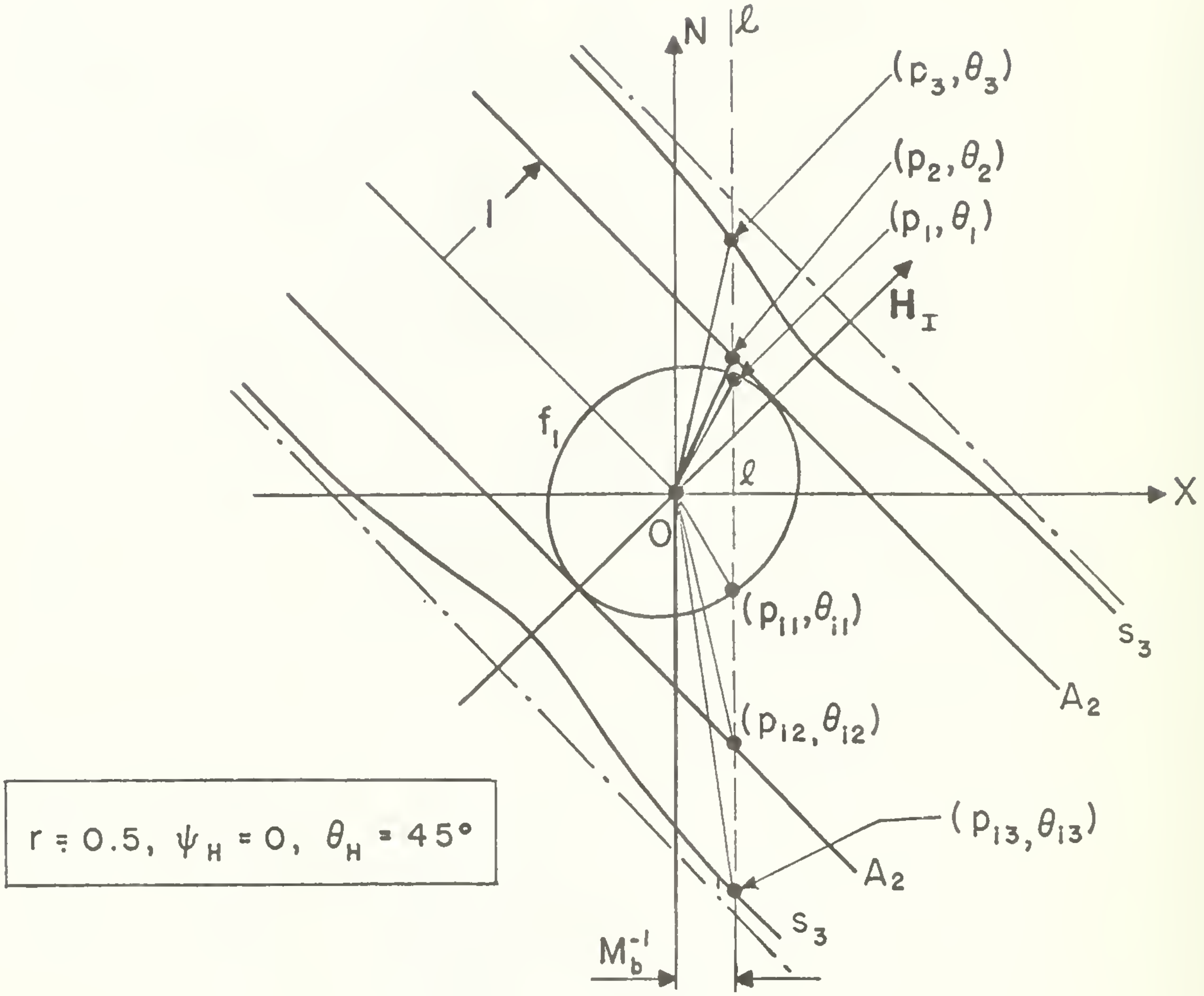

Figure 9 (a) Graphical determination of the angles of reflection. All angles are measured from the vertical axis. Clockwise angles are regarded positive, counterclockwise angles negative. The angles of reflection $\theta_{ij}$, $j = 1,2,3$ corresponding to an angle of incidence $\theta_i$, of a front of type i are obtained by finding the intersections of the line ℓ with the portions of s, A and f curves that lie beneath the x-axis.

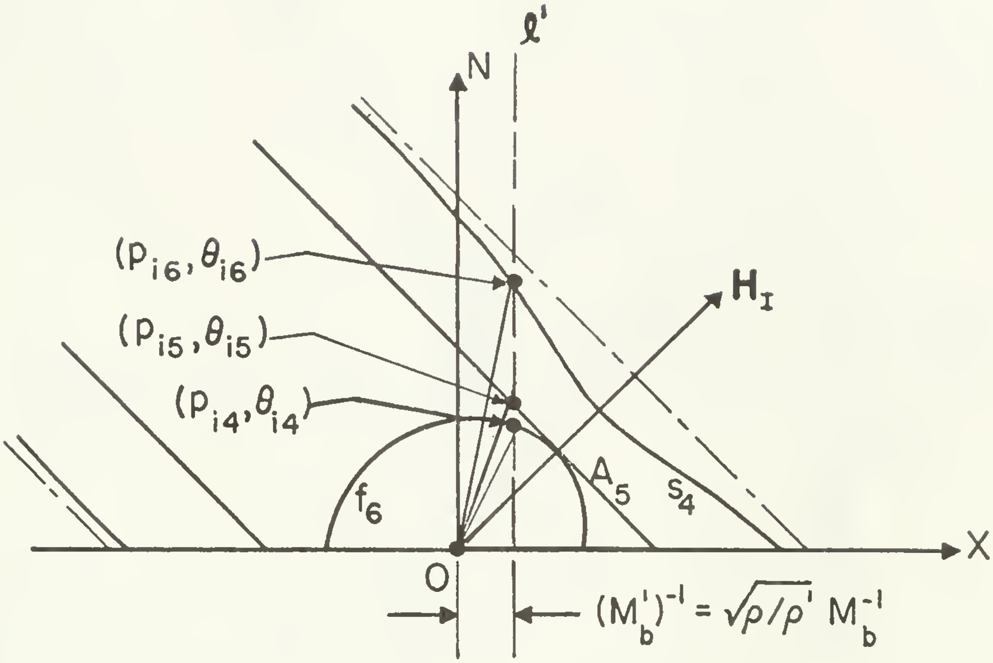

Figure 9. (b) Graphical determination of the angles of refraction corresponding to an angle of incidence $\theta_i$ of a front of type i. The figure is identical with the upper portion of Figure 8(a). However, the line $\ell'$ that determines the angles of refraction is closer to or further from the vertical axis than is $\ell$ according as the square root of the density ratio is less than or greater than unity.

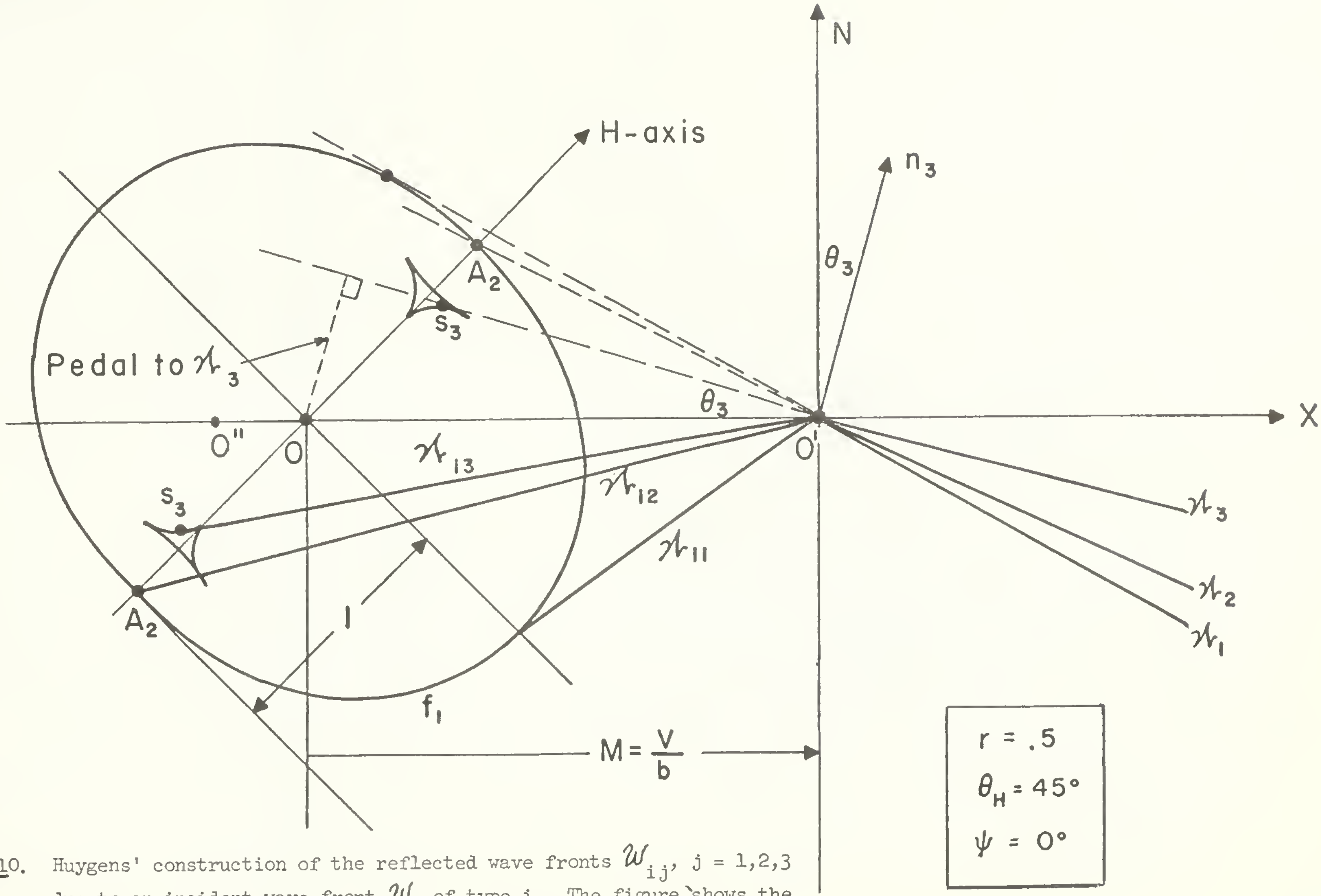

Figure 10. Huygens' construction of the reflected wave fronts $\mathcal{W}_{ij}$, $j = 1,2,3$ due to an incident wave front $\mathcal{W}_i$ of type i. The figure shows the "wavelet" emerging from O this point having been excited $b^{-1}$ seconds before the instant depicted. The dashed extension of $\mathcal{W}_i$ are tangent to the upper hemisphere while the corresponding reflected fronts are tangent to the lower hemisphere.

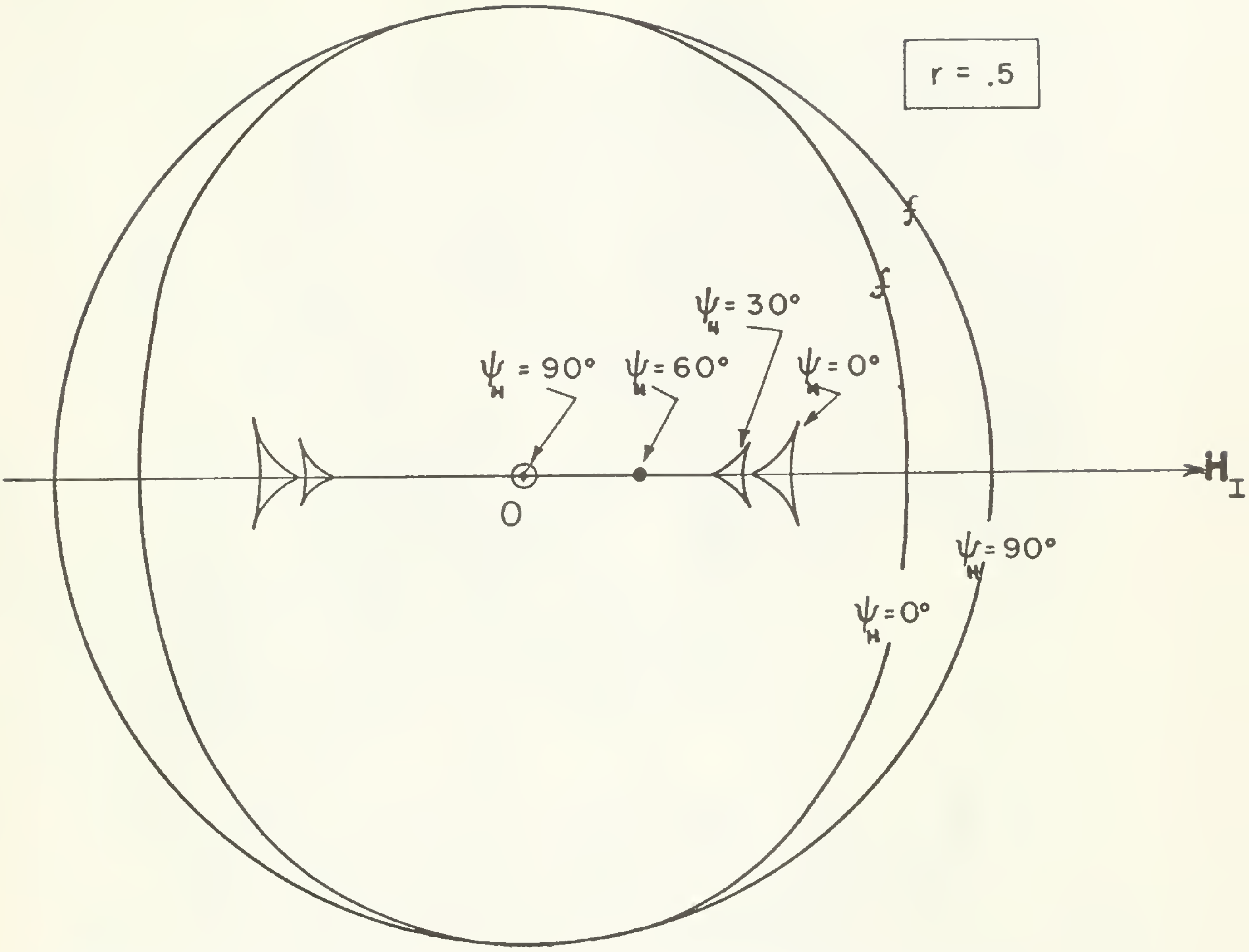

Figure 11. The projection onto the plane of incidence of those curves on the Friedrichs' ray surface at all points of which the surface normal is parallel to the plane of incidence. The parameters r and $\theta_H$ are .5 and $0^\circ$ respectively. The variable parameter is $\psi_H$.

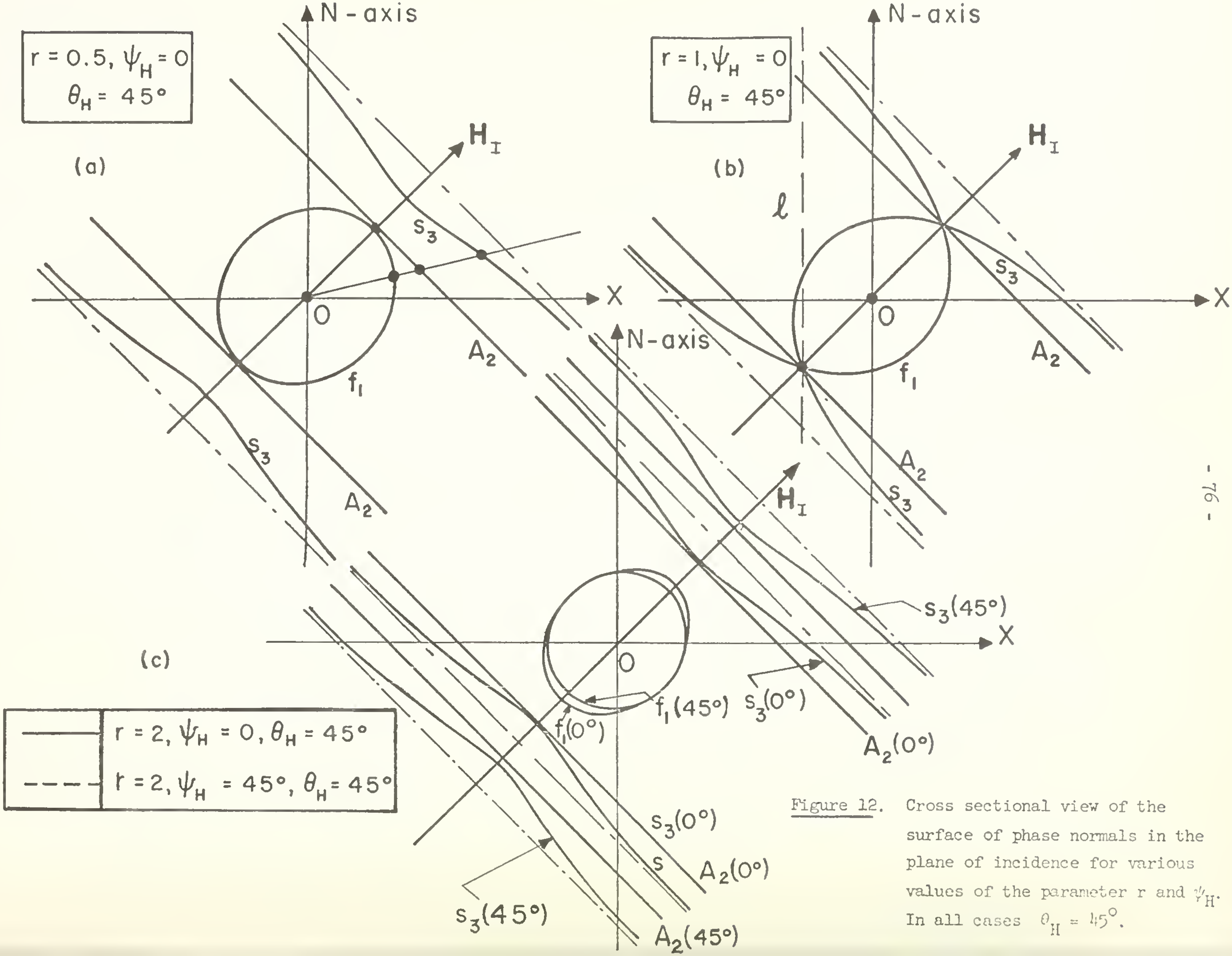

Figure 12. Cross sectional view of the surface of phase normals in the plane of incidence for various values of the parameter r and $\psi_H$. In all cases $\theta_H = 45^\circ$.

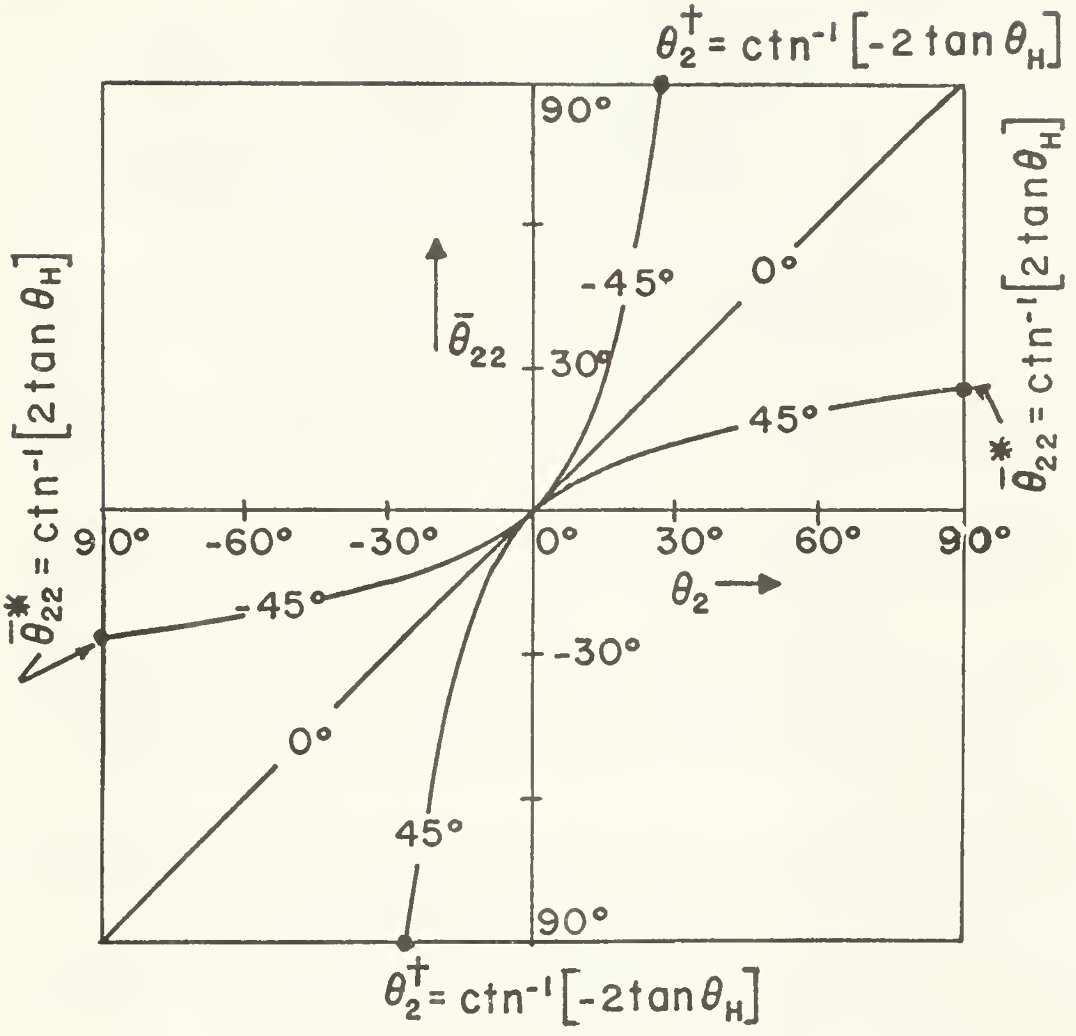

Figure 13. Plots of the (acute) angle of reflection $\theta_{22}$ against $\theta_2$ for the parameter values $\theta_H = 0^\circ$, and ± 45°.

# REFERENCES

[1] J. Bazer and O. W. Fleischman

  (a) Propagation of weak hydromagnetic discontinuities, Report No. MH-10, (1959)

  (b) Propagation of weak hydromagnetic discontinuities, Phys. Fluids, 2, (1959).

[2] F. G. Friedlander,

  (a) Simple progressive solutions of the wave equation, Proc. Camb. Phil. Soc., 43 (1956).

  (b) Sound pulses in a conducting medium, Proc. Camb. Phil. Soc. 55 p. 341-367 (1959).

[3] D. Ludwig, Exact and Asymptotic Solutions of the Cauchy Problem, Communs. Pure and Appl. Math. 13 (1960).

[4] R. K. Luneberg, Mathematical theory of optics, (Lecture notes) Brown University (1944); Propagation of electromagnetic waves (Lecture notes) New York University, (1949).

[5] M. Kline,

  (a) An asymptotic solution of Maxwell's equations, Comm. Pure Appl. Math IV, pp. 225-263, (1951).

  (b) Asymptotic solution of linear hyperbolic partial differential equations, J. Rational Mech. Anal., 3, (1954).

  (c) Electromagnetic Waves, University of Wisconsin Press, Madison, (1962).

[6] J. B. Keller,

  (a) Geometrical Theory of Diffraction, J. Opt. Soc. Am., 52, 116-130, (1961). The reader is referred to this survey article and to the references cited therein.

  (b) Geometrical acoustics, J. Appl. Phys. 25, 938, (1954).

[7] V. C. A. Ferraro, Reflection and refraction of hydromagnetic Waves, Astrophy. J. 119 (1954).

[8] N. Herlofson, Magneto-hydrodynamic waves in a compressible fluid conductor, Nature 165, 1020, (1950).

[9] H. C. van de Hulst, Interstellar polarization and magneto-hydrodynamic waves, Appeared in Problems of Cosmical Aerodynamics, p. 46 (Int. Union of Theor. and Appl. Mech. and Int. Astr. Union Proc. Symposium Paris, (1949)). Published by Central Air Documents Office, Dayton, Ohio, (1951).

[10] S. Lundquist, Studies in magneto-hydrodynamics, Arkiv Fysik, 5, (1952).

[11] A. Baños, Jr. Fundamental Wave Functions in an unbounded magneto-hydrodynamic field I. General Theory, Phys. Rev. 97, 1435-43, (1955).

[12] M. J. Lighthill, Studies on magneto-hydrodynamic waves and other anisotropic wave motions, Phil. Trans. Roy. Soc. 252 397-430, (1960).

[13] K. O. Friedrichs, Nonlinear Wave Motion in magnetohydrodynamics Los Alamos report No. 2105 (written 1954, distributed 1957).

[14] K. O. Friedrichs and H. Kranzer, Notes on magnetohydrodynamics, MH-VIII, Inst. Math. Sci. N.Y.U., (1958).

[15] H. Grad, Propagation of magnetohydordynamic waves without radial alternation. Appeared in The Magnetodynamics of Conducting Fluids, edited by D. Bershader, pp. 37-60. Stanford University Press, (1959).

[16] G. J. F. MacDonald, Spectrum of Hydromagnetic Waves in the Exosphere; J. Geophys. Research 66, 3639, (1961).

[17] A. J. Dessler and E. N. Parker, Hydromagnetic theory of geomagnetic storms, J. Geophys. Research 64 2239-2252, (1959).

[18] R. Courant and P. D. Lax, The propagation of discontinuities in wave motion. Proc. Nat. Acad. Sci. 42, 872-876, (1956).

[19] R. Lewis, Discontinuous initial value problems for symmetric hyperbolic linear differential equations. J. of Math. and Mech., 7, 571-592, (1958).

[20] P. D. Lax, Asymptotic solutions of oscillatory initial value problems, Duke Math. J. 24, 627-646, (1957).

[21] H. Weitzner, Green's function for two-dimensional magnetohydrodynamic waves, I, II, Phys. Fluids, 4, (1961).

[22] J. Bazer, Reflection and refraction of weak hydromagnetic discontinuities, Research Report No. MH-11, Division of Electromagnetic Research, Courant Institute of Mathematical Sciences (1961).

[23] P. H. Roberts, On the reflection and refraction of hydromagnetic waves, Astrophys. J. 121, 720-730, (1955).

[24] K. Pearson, Tables of the Incomplete Beta Function, BIOMETRIKA OFFICE: Univ. College, London (1934).

[25] W. E. Francis, M. I. Green, and A. J. Dessler, Hydromagnetic propagation of sudden commencements of magnetic storms; J. Geophys. Research, 64, p. 1643 (1959).

[26] G. Schubert, Linearized oscillations in a plasma, Graduate School of Aeronautical Engineering, Cornell University AFOSR 1026, (1961).

[27] H. Grad and M. Rose, Notes on Magnetohydrodynamics I, II, and III, Report No. NYO 6486, Courant Institute of Mathematical Sciences, N. Y. U. (1956).

[28] R. Liboff, Propagation of Long Wavelength Disturbances in a Plasma, Report No. NYO 9762, Courant Institute of Mathematical Sciences, N. Y. U. (1961).

[29] L. Schwartz, Theorie des distributions, Vols. 1 and 2, Hermann of (i.e., Paris, 1950-51).

NOV 26 1962

DATE DUE

DEC 17 '63
DEC 23 '65
FEB 27 1980
NOV 3 1987
JAN [illegible] 1988

GAYLORD
PRINTED IN U.S.A.

NYU
EM-
176
Bazer
c.1

Geometrical hydromagnetics.

NYU
EM-176
Bazer
c.1
AUTHOR
Geometrical hydromagnetics
TITLE

| DATE DUE | BORROWER'S NAME | ROOM NUMBER |
|---|---|---|
| DEC 17 '63 | ~~Gary S. Doon~~ | |
| ~~[illegible] 63~~ | ~~D. [illegible]~~ | |
| | ~~SAMPERI~~ | |
| JAN 30 [illegible] | [illegible] | |

N. Y. U. Courant Institute of
Mathematical Sciences
4 Washington Place
New York 3, N. Y.